

Sudan University of Science and Technology
College of Graduate Studies



Coherence and Stochastic Resonances in Chaotic Semiconductor Lasers

رنين الترابط والرنين العشوائي في ليزرات أشباه الموصلات
المُشوشة

A Thesis Submitted in Fulfillment of the Requirements
for the Degree of Doctor of Philosophy in Laser
Applications in Physics.

By

Ibrahim Hamad Gabier Mohammed

Supervisor

Prof: Kais AbdElsatar Alnaimee

Co- Supervisor

Dr: Abdelmoneim Mohammed Awadelgied

February 2016

الآية

بِسْمِ اللَّهِ الرَّحْمَنِ الرَّحِيمِ

قال تعالى:

وَإِنْ تَعُدُّوا نِعْمَةَ اللَّهِ لَا تُحْصُوهَا إِنَّ اللَّهَ لَعَفُورٌ رَحِيمٌ (18).

سورة النحل

Dedication

This thesis is dedicated to:

My parents' soul, who infused the
streak of hope at me to pursue my aim,

My wife Moniera, my best associate
through every life.

My sons for their patience.

Acknowledgement

I express my deep sense of thankfulness to my supervisor Prof.Kais Al-Naimee, for his consistent guidance and intellectual support which helped me to complete my research work successfully and submit the thesis in time. I can't forget how he found time to spend with me- however busy he was- to go through my results, correct them and give suggestions for future works.

I am grateful to my co-supervisor Dr.Abdelmoneim Awadelgied for his support and encouragement throughout my research career; he always boosted my energy levels with his positive thoughts and pleasant behavior whenever I was about to be depressed.

Thanks to Dr. Sora Abdalah for her valuable advices and fruitful discussions which always created turning points in my research.

I also thank Dr. Wafa Salih for her timely advices. And my thanks extend to other staff and students of laser Institute laser.

I thank my friends at Institute of laser for their affection and timely help which made my study days unforgettable specially (Abou- Asha and Naser Saeed).

I am also thankful the library staff in Institute of laser for their love, and support which helped a lot for the successful accomplished of my research.

Abstract

In the last three decades a plethora of works has been devoted to study both stochastic coherence (SC) and stochastic resonances (SR) phenomena in chaotic dynamical systems.

In this work we experimentally investigated the route to chaos in stable dynamical laser diode system via optoelectronic feedback, SC or CR and SR phenomena. Our work consists of three phases:

Firstly: we report the experimental evidence the spiking generation in semiconductor laser with a closed loop ac-coupled optoelectronic feedback. The results show that when the feedback strength fixed in a certain value and fluctuating the values of the bias current, stability in chaotic regime decreases towards unstable behavior.

At a given laser bias current value with changing in the feedback strength, the behavior of the stability laser diode regime displayed sequence gradation from stable, quasi-stable and chaotic states.

The results declare that optoelectronic feedback is one of the important routes to the chaos, through the perturbations of bias current (δ) or feedback strength (ϵ) as control parameters.

Secondly: we show that dynamical nonlinear chaotic laser diode (LD) system, can display the main feature of coherence resonance, in particular the presence of noise signal exhibits oscillations whose regularity is optimal for some intermediate value of the noise intensity (D).

Finally: we observed that a dynamical chaotic system of (LD) driven to both periodic weak forcing (signal) and random perturbation (white noise) sequentially, shows a resonance (peak in the power spectrum)

where that peak is absent whenever either the forcing or the perturbation is absent, this feature so call stochastic resonance (SR).

The presence of the noise becomes beneficial to signal up to a point where an increase of the noise improves the performance for transmitting or detecting the signal.

At the end of this work, we summarized all the results obtained from this work, and also we suggested some works for future in the field of semiconductor laser applications.

المستخلص

خلال العقود الثلاثة الأخيرة كُرسَتْ وفرة من الأعمال لدراسة كلاً من ظاهرتي رنين الترابط والرنين العشوائي في الأنظمة الديناميكية المشوشة.

في هذا البحث تم التحقق عملياً من أن التغذية الخلفية (التعليقات) الكهروضوئية، هي طريقة لتوليد الشواش في نظام ليزر الثنائي المستقر وكذلك تمت دراسة ظاهرة رنين الترابط و العشوائي عملياً.

جاء هذا البحث مشتملاً علي ثلاث مراحل هي :-

أولاً: وجد بالدليل التجريبي أنه يمكن توليد نبذبات في ليزر الثنائي خلال حلقة مغلقة للتيار المباشر وموصله بالتعليقات الكهروضوئية.

أوضحت النتائج أن إستقرارية سلوك النظام الليزري الفوضوي تتناقص نحو السلوك الغير مستقر عندما تكون التعليقات الكهروضوئية ثابتة القيمة بينما تكون شدة تيار الإنحياز متغيرة. كما أوضحت النتائج أيضاً في حالة ثبوت شدة التيار عند قيمة معينة وتغيير قيم التعليق ات فإن النظام أظهر تدريجاً متعاقباً من الحالة المستقرة إلي الحالة الشبه المستقرة إلي الحالة الفوضوية.

ثانياً: تم التوصل إلي ان النظام الديناميكي اللاخطي الفوضوي في حالة ليزر الثنائي يظهر الملامح الرئيسة لظاهرة ترد الترابط ، وبالتحديد فإن وجود إشارة الضوضاء يولد ذروات(قمم) ذات إنتظام تام عند القيمة المثالية لشدة الضوضاء.

أخيراً عندما تطبق إشارة دورية ضعيفة فقط في النظام الديناميكي الفوضوي، ومن ثم تضاف إشارة الضوضاء فإنه يتولد في النظام ظاهرة الرنين العشوائي ذروة (قمة) في طيف خرج الليزر وتختفي هذه الذروة باختفاء الإشارة الدورية أو إشارة الضوضاء.

أوضحت النتائج أن إشارة الضوضاء تكون مدعمة للإشارة الدورية إلي النقطة التي تكون عندها قيمة الضوضاء مثالية بحيث تعمل في تحسين الأداء لإرسال أو إكتشاف الإشارة.

في نهاية هذا العمل تم تلخيص كل النتائج التي تم الحصول عليها من هذا العمل، وكذلك
أُتُرحت بعض المواضيع من أجل القيام بها في المستقبل في مجال تطبيقات أنظمة ليزرات أشباه
الموصلات.

Contents

Dedication.....	I
Acknowledgement.....	II
Abstract.....	III
المستخلص.....	V
Table of Contents.....	VII
List of Figures.....	XI
List of Tables.....	XVI
Chapter One	Introduction and Basic Concepts
1.1 Introduction.....	1
1.2 The aim of this work.....	2
1.3 Chaos.....	2
1.3.1 Chaos Background and Definition.....	2
1.3.2 Attractors.....	6
1.4 Chaos Analysis Tools.....	10
1.4.1 The Bursting.....	10
1.4.2 Attractor in Phase Space.....	11
1.4.3 Bifurcation Diagram.....	13
1.5 Time Series.....	15
1.6 Fast Fourier Transformation (FFT).....	15
1.7 The Feedback in Dynamic Systems.....	16
1.8 Chaos Generation in Semiconductor Laser System.....	17
1.8.1 Laser Diode with Optical Injection.....	17
1.8.2 Laser Diode with Optical Feedback.....	18
1.8.3 Laser Diode with Optoelectronic Feedback.....	18

1.9 Diode Lasers-----	20
1.10 Fiber Optic Transceiver-----	21
1.10.1 Fiber Optic Transmitters-----	22
1.10.2 The Receivers' Information-----	23
1.11 Thesis Layout-----	23
Chapter Two	Noise, Coherence and Stochastic Resonance
2.1 Introduction-----	24
2.2 Types of Noise-----	25
2.2.1 Thermal Noise-----	25
2.2.2 Shot Noise-----	27
2.2.3 Low Frequency Noise-----	27
2.2.4 White Noise-----	29
2.3 Coherence Resonance (CR) in Chaotic Systems-----	29
2.4 Stochastic Resonance (SR) in Chaotic Systems-----	32
2.4.1 The Single - to - Noise Ratio (SNR)-----	33
2.4.2 The Mechanism of the Stochastic Resonance-----	33
2.4.3 A simple Model of Stochastic Resonance-----	35
2.4.4 Applications of Stochastic and Coherence Resonance-----	38
2.4.4.1 Neuroscience-----	39
2.4.4.2 Medicine-----	39
2.4.4.3 Signal analysis-----	39
2.5 Literature Review-----	40

Chapter Three	the Experimental Part	
3.1 Introduction		46
3.2 The Equipment		46
3.2.1 DC Power Supply		46
3.2.2 Optical Transmitter		47
3.2.3 Optical fiber		48
3.2.4 Optical Receiver		49
3.2.5 Analog Oscilloscope		50
3.2.6 Digital Oscilloscope		51
3.2.7 Function generator		52
3.2.8 The White Noise generator		53
3.3 The Experimental setup		54
3.4 The Method		56
3.5 Coherence Resonance		58
3.6 Stochastic Resonance		59
3.7 Dynamical model		59
Chapter Four	Results, Discussion and Conclusion	
4.1 Introduction		62
4.2 The Experimental Results		63
4.2.1 Optoelectronic chaotic dynamics		63
4.2.1.1 The influences of variable Bias current on the chaos state		63
4.2.1.2 The Influences of Variable Feedback Strength on Chaos state..		68
4.2.1.3 Effect of Modulation on the Chaotic System		73
4.2.2 The Influences of Noise on the Chaotic System Behavior		74
4.2.2.1 Coherence Resonance Phenomenon		74

4.2.2.2 Stochastic Resonance Phenomenon-----	80
4.3 Conclusion-----	85
4.4 Suggestion for Future work-----	86
Reference-----	87

List of Figures

Figure No.	Title of figure	Page No.
<i>Figure (1.1)</i>	<i>The butterfly effect.</i>	6
<i>Figure (1.2)</i>	<i>Schematic of attractors.</i>	6
<i>Figure (1.3)</i>	<i>The Lorenz attractor. Two solutions with initial conditions.</i>	7
<i>Figure (1.4)</i>	<i>The Rossler attractor.</i>	8
<i>Figure(1.5)</i>	<i>Numerically calculated time series (left row), attractors (middle row), and power spectra (right row) for different feedback ratios.</i>	9
<i>Figure (1.6)</i>	<i>the neural burst signal showing the duty cycle, active phase and inters pike, interburst, quiescent periods.</i>	11
<i>Figure(1.7)</i>	<i>Shows the bifurcation Diagram of the logistic map, r along the x-axis between 0 and 4.</i>	13
<i>Figure (1.8)</i>	<i>Shows the bifurcation Diagram of the logistic map, r along the x-axis between 3.4 and 4.</i>	14
<i>Figure (1.9)</i>	<i>Saddle-node bifurcation as r varied.</i>	15
<i>Figure:(1.10)</i>	<i>Block diagram form the idea of feedback.</i>	16
<i>Figure 1.11</i>	<i>Schematic diagram of laser diode with optical feedback.</i>	18
<i>Figure 1.12</i>	<i>Schematic diagram of laser diode with optical feedback.</i>	19

Fig. 1.13	Schematic diagram of laser diode with delayed optoelectronic feedback.	20
Figure(1.14)	Fiber optic transceiver block diagram.	21
Figure(1.15)	Single mode vs. Multimode fiber.	22
Fig: 2.1	Thermal noise signal as seen on an oscilloscope trace.	26
Figure (2.2)	Johnson noise models.	27
Figure:(2.3)	The dynamics of the Fitz Hugh–Nagumo system [Eqs. (6), (7)] for $\alpha = 1.05$, $\varepsilon = 0.01$, $D = 0.02$.	31
Figure (2.4)	Coherence Resonance principle: proper noise intensity optimizes the periodicity of the system output.	32
Figure (2.5)	A general scheme for stochastic resonance.	34
Figure (2.6)	Sketch of the double- well the minima are located at $x \pm 1$.	36
Figure (2.7)	Single realizations of $x(t)$ in the periodically modulated double well potential, for three different values of the noise strength, D .	38
Figure (3.1)	shows the photograph of the DC power supply 30V/5A	47
Figure (3.2)	The schematic face view of optical transmitter.	48
Figure (3.3)	An optical receiver.	50
Figure (3.4)	Analog Oscilloscope HM 1004-3.	51
Figure (3.5)	TDS2012c Two channel digital storage oscilloscope photograph.	52
Figure (3.6)	Front view of the Function generator Order NO: 13652.93.	53
Figure (3.7)	Front view of the white noise generator.	54

Figure (3.8-a)	Schematic experimental setup for chaotic generation	55
Figure (3.8-b)	Photographic experimental setup for chaotic generation	55
Figure (3.8-c)	Experimental setup photographic with the waveform generator.	57
Figure (3.9)	Experimental Setup of Coherency	58
Figure (3.10)	Experimental Setup of Stochastic Resonance Procedures.	59
Figure (4.1)	(a) Experimental time series of system at $\delta_o = 4.1\text{mA}$, (b) the corresponding attractor, (c) the corresponding FFT.	64
Figure (4.2)	(a) Experimental time series of system at $\delta_o = 5.8\text{mA}$, (b) the corresponding attractor, (c) the corresponding FFT.	65
Figure 4.3:	(a) Experimental time series of system at $\delta_o = 8.2\text{mA}$, (b) the corresponding attractor, (c) the corresponding FFT.	66
Figure (4.4)	(a) Experimental time series of system when $\delta_o = 9\text{mA}$ (b) the corresponding attractor, (c) the corresponding FFT.	67
Figure (4.5)	Bifurcation diagrams (maxima of photon densities vs bias current as a control parameter.).	68
Figure (4.6)	(a) The time series when $\varepsilon = 0.78$, (b) the corresponding FFT (c) the corresponding attractor.	69
Figure (4.7)	(a) The time series when $\varepsilon = 0.82$, (b) the corresponding FFT (c) the corresponding attractor.	70

Figure (4.8)	(a) The time series when $\varepsilon = 0.94$, (c) the corresponding FFT, (b) the corresponding phase space (attractor).	71
Figure (4.9)	(a) The time series when $\varepsilon = 1.32$, (b) the corresponding FFT, (c) the corresponding attractor.	72
Figure (4.10)	Experimental bifurcation diagram of the laser intensity as a function of the frequency modulation.	73
Figure (4.11)	(a) Experimental time series of the semiconductor laser with feedback, (b) the corresponding Trajectory at noise of $D = 5.5\text{mV}$.	75
Figure (4.12)	(a) Experimental time series of the semiconductor laser with feedback, (b) the corresponding Trajectory at noise of $D = 9.5\text{mV}$.	75
Figure (4.13)	(a) Experimental time series of the semiconductor laser with feedback, (b) the corresponding Trajectory at noise of $D = 12.5\text{mV}$.	76
Figure (4.14)	(a) Experimental time series of the semiconductor laser with feedback, (b) the corresponding Trajectory at noise of $D = 25.5\text{mV}$.	77
Figure (4.15)	Experimental bifurcation diagrams as a function of noise intensity.	77

<i>Figure (4.16)</i>	<i>The coefficient of variation R as a function of noise intensity.</i>	78
<i>Figure (4.17)</i>	<i>SNR as a function of noise intensity shows the coherence resonance at optimal noise intensity.</i>	80
<i>Figure (4.18)</i>	<i>Sinusoidal signal was modulated to the feedback loop with a noise signal.</i>	81
<i>Figure (4.19)</i>	<i>The increasing of the signal power spectrum as a function of the values of noise intensity.</i>	83
<i>Figure (4.20)</i>	<i>Experimental results for the signal to noise ratio as a function of the noise value.</i>	84

List of Tables

Table No.	Title of Table	Page No.
<i>Table (3.1)</i>	<i>Shows Characteristics of the DC Power Supply 30V/5A</i>	47
<i>Table (3.2)</i>	<i>The optical fiber specifications.</i>	49
<i>Table (3.3)</i>	<i>The specifications of the digital oscilloscope.</i>	51
<i>Table (3.4)</i>	<i>The specification of function generation.</i>	52-53
<i>Table (4.1)</i>	<i>The Experimental values of noise intensity and NSR in the CR effect respectively.</i>	79
<i>Table (4.2)</i>	<i>The Experimental values of noise intensity and NSR in SR effect respectively.</i>	84

CHAPTER ONE

Introduction and basic concepts

1.1 Introduction

A nonlinear system is one that does not satisfy the superposition principle, or one whose output is not directly proportional to its input; but a linear system fulfills these conditions (Abdalah, 2013), in other words, a nonlinear system is any problem where the variable(s) to be solved for, cannot be written as a linear combination of independent components. Nonlinear problems are of interest to engineers, physicists and mathematicians because most physical systems are inherently nonlinear in nature. Nonlinear equations are difficult to solve and give rise to interesting phenomena such as chaos. Some aspects of the weather (although not the climate) are seen to be chaotic, where simple changes in one part of the system produces complex effects throughout. A nonlinear system is not random (Abdalah, 2013).

Nature is complex. It features a multitude of systems which, though they may be simple, are unpredictable in their behavior, and seem not to be governed by the established deterministic laws of classical physics.

For many years, scientists ignored such systems claiming that their unpredictability was a result of the limitations in the accuracy of measurements or pure chance. Others even rejected them as unscientific. However, in the 1970s, a new theory evolved, which, if its supporters are right, explains the diversity we observe in nature and provides an accurate

and scientific description of the unpredictable phenomena in question. This is known as “Chaos Theory”; which is a field of study in mathematics, with applications in several disciplines including physics, engineering, economics, biology, philosophy, geology, computer science, politics, population dynamics, psychology and robotics. Chaos theory studies the behavior of dynamical systems that are highly sensitive to initial conditions (external forces) (Csele, 2004, and Abdalah, 2013).

1.2 The aim of this work

This work aimed to generate a chaos signal in a non-linear dynamical system by means of photo-current feedback (electro-optical feedback); also it aimed to control the behavior of the chaotic system via the noise. And to study the stochastic coherence (SC) or coherence resonance (CR) and stochastic resonance (SR) phenomena in chaotic non-linear dynamics systems, by using noise only or with an external signal.

1.3 Chaos

1.3.1 Chaos Background and Definitions

Chaos theory is applied in many scientific disciplines: mathematics, programming, microbiology, biology, computer, science, economics, engineering, finance, philosophy, physics, politics, population dynamics, psychology, and robotics (Tredicce, et al., 1985).

Chaos occurs in optics, both in lasers and in nonlinear optical devices. Such systems, which are fundamentally simple both in construction and in the mathematics that describe them, provide excellent opportunities for investigating these nonlinear phenomena as well as for technological innovation (Abdalah, Al-Naimee, and Meucci, 2010).

Chaotic behavior of a dynamic system has (a) a very large (possibly infinite) number of attractors (a set of values in the phase space to whom the system migrates over time, or iterations). And (b) is sensitive to initial conditions. Sensitivity to initial conditions means that each point in such a system is arbitrarily closely approximated by other points with significantly different future trajectories. Thus, an arbitrarily small perturbation of the current trajectory may lead to significantly different future behavior (Areechi, Meucci, and Gadomski, 1986).

There are many possible definitions of chaos. In fact, there is no general agreement within the scientific community as to what constitutes a chaotic dynamical system] (Scholl, and Schuster, 2008).

W.G.Flake defined Chaos as an Irregular motion of a dynamical system that is deterministic, sensitive to initial conditions, and impossible to predict in the long term with anything less than an infinite and perfect representation of analog values(Rontani, and Citrin, 2005). But G.P. Williams defined Chaos as sustained and disorderly-looking long-term evolution that satisfies certain special mathematical criteria and that occurs in a deterministic non-linear system (Rontani, and Citrin, 2005). While E. Lorenz defined chaos as the property that characterizes a dynamical system in which most orbits exhibit sensitive dependence (Rontani, and Citrin, 2005).

Another definition of chaos is a type of unpredictable motion generated by deterministic differential equations, rules which generate chaos are called chaotic dynamical systems, and the space used to describe a system is often called the phase space (Kaneko, and Tsuda, 2001).

Chaos is an inherent feature of many nonlinear systems. In particular, the transition from order to disorder occurs with universality, irrespective of

physical properties of the systems (Abdalah, Al-Naimee, and Meucci, 2010).

The original meaning of chaos is a total disorder and ultimate unpredictability (Abraham, and Ueda, 2000, Zhang, Liu, and Wang, 2009).

In most of definitions chaotic processes are treated as solutions of nonlinear differential or difference equations, characterized by local instability and global boundedness. It means that solutions with close initial conditions will diverge to some finite distance after some time (so called sensitive dependence on initial conditions). Difference equations describe the evolution of system in continuous time (Strogatz, 1994).

Chaotic behavior has been observed in the laboratory in a variety of systems including electrical circuits, lasers, oscillating chemical reactions, fluid dynamics, and mechanical and magneto-mechanical devices, as well as computer models of chaotic processes. Observations of chaotic behavior in nature include changes in weather, the dynamics of satellites in the solar system, the time evolution of the magnetic field of celestial bodies, population growth in ecology, the dynamics of the action potentials in neurons, and molecular vibrations. There is some controversy over the existence of chaotic dynamics in plate tectonics and in economics. One of the most successful applications of chaos theory has been in ecology, where dynamical systems such as the Ricker model have been used to show how population growth under density dependence can lead to chaotic dynamics. Chaos theory is also currently being applied to medical studies of epilepsy, specifically to the prediction of seemingly random seizures by observing initial conditions. A related field of physics called quantum chaos theory investigates the relationship between chaos and quantum mechanics. The correspondence principle states that classical mechanics is a special case of quantum mechanics, the classical limit. If quantum

mechanics does not demonstrate an exponential sensitivity to initial conditions, it is unclear how exponential sensitivity to initial conditions can arise in practice in classical chaos. Recently, another field, called relativistic chaos, has emerged to describe systems that follow the laws of general relativity. The initial conditions of three or more bodies interacting through gravitational attraction (see the n-body problem) can be arranged to produce chaotic motion (Strogatz, 1994, Alice Project, 1994).

In chaos theory, the butterfly effect is the sensitive dependence on initial conditions; where a small change at one place in a nonlinear system can result in large differences to a later state. The effect derives its name from the theoretical example of a hurricane's formation being contingent on whether or not a distant butterfly had flapped its wings several weeks before (Alice Project, 1994).

The butterfly effect stipulates that "any act, despite the seeming simplicity of the apparently has influence and may develop this effect developed dramatically unexpected so that the butterfly's wings flap in California would lead to hurricanes and storms in China, after years!" And meaning that flutter butterfly's wings can cause a slight change in the universe (weather) starting and pitching to a series of events and lead to many changes in the end. The figure below shows the shape of butterfly effect:

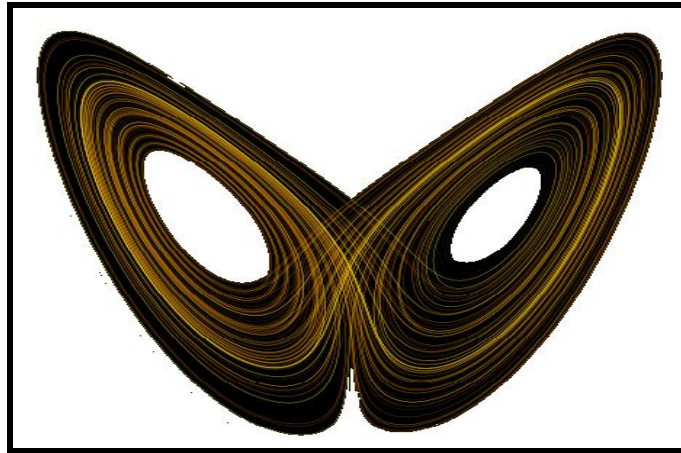


Figure (1.1): the butterfly effect.

1.3.2 Attractors

An attractor is a set of values in the phase space to which a system migrates over time, or iterations. It need not be one- or two-dimensional. Attractors can have as many dimensions as the number of variables that influence its system (Scholl, and Schuster, 2008). The chaotic attractor in phase space is densely sampled by an infinite number of unstable periodic orbits (Liu, and Ohtsubo, 1994). A range of possible attractors can be shown in figure 2.2. The attractors can either be: (a) fixed point, which represents a stable constant output, (b) a limit- cycle, which represents a periodic oscillation, (c) torus, which represents a quasi-periodic output power and (d) chaotic, which represents output power fluctuating chaotically (Mork, Tromborg, and Mark, 1992).

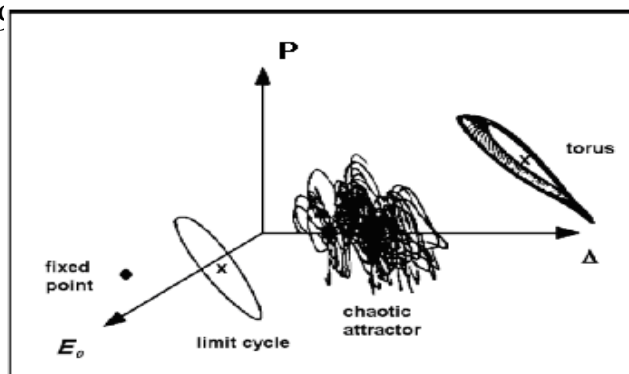


Figure: (1.2) Schematic of attractors (Mork, Tromborg, and Mark, 1992).

A fixed point is a point of a function that does not change under some transformation. A limit cycle is an attractor that is periodic in time, that is, cycles periodically through an ordered sequence of states. A torus is an attractor consisting of N independent oscillations, plotted in phase space (Clayton, 1997).

A strange attractor is an attractor which has non-integer dimension, or the dynamics on it are chaotic. Lorenz attractor is a butterfly-shaped strange attractor. It came from a meteorological model developed by Edward Lorenz in 1963 with three equations and three variables. It was one of the first strange attractors studied (Clayton, 1997).

. The system of differential equations involved only two nonlinear terms and was given by: (Hirsch, Smale, and Devaney 2004).

$$\begin{aligned} x' &= u(y - x) \\ y' &= Dx - y - xz \dots\dots\dots(1.1) \\ z' &= xy - qz. \end{aligned}$$

Where u, D, and q are positive parameters and, moreover, $\sigma > b + 1$, as in figure 1.3.

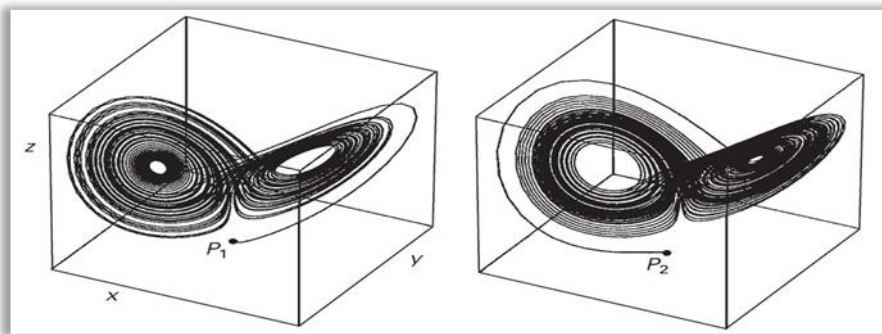


Figure: (1.3) the Lorenz attractor. Two solutions with initial conditions $P_1 = (0, 2, 0)$ and $P_2 = (0, -2, 0)$, (Hirsch, Smale , And Devaney , 2004).

The solution curves were displayed through two different initial conditions:

$P1 = (0, 2, 0)$ and $P2 = (0, -2, 0)$ when the parameters are: $\sigma = 10$, $b = 8/3$, and $r = 28$. These are the original parameters that led to Lorenz's discovery. It can be noted how both solutions start out very differently, but eventually have more or less the same fate, they both seem to wind around a pair of points, alternating at times which point they encircle. This is the first important fact about the Lorenz system: All non equilibrium solutions tend eventually to the same complicated set, the so-called Lorenz attractor.

The Rossler system, it is a three-dimensional system similar in many respects to the Lorenz system. is given by:(Abdalah, Al-Naimee, and Meucci, 2010).

$$\begin{aligned} x' &= -y - z \\ y' &= x + ay \dots\dots\dots (1.2) \\ z' &= b + z(x - C) \end{aligned}$$

where a , b , and C are real parameters, as shown in figure 1.4

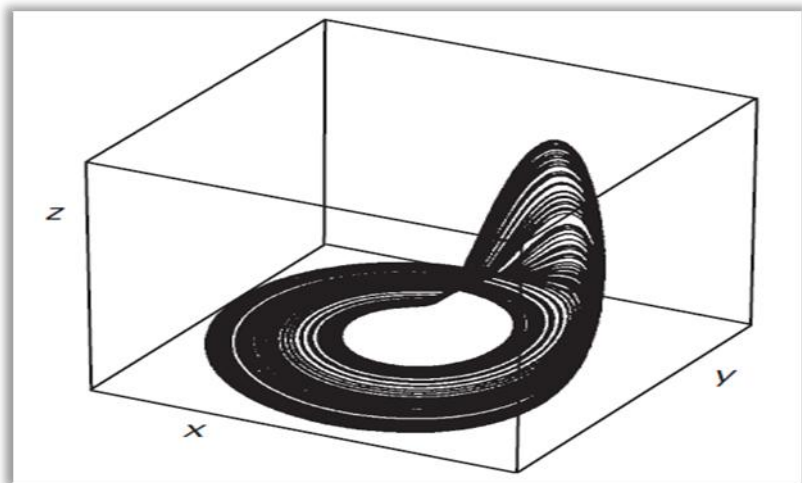


Figure :(1.4) The Rossler attractor (Hirsch, Smale , And Devaney , 2004).

For simplicity, the case where $a = 1/4$, $b = 1$, and c ranges from 0 to 7, as with the Lorenz system, it is difficult to prove specific results about this system. A chaotic attractor is a trajectory in the phase space of chaotic variables and is frequently used of the analysis of chaotic oscillations (Ohtsubo, 2008). Since the laser output power at a stable oscillation is

constant, the attractor is a fixed point in the phase space of the output power and the carrier density. A period-1 signal, as the case in figure 1.5(a), is a closed loop. The attractor of a period-2 oscillation is a double-loop as shown in figure 1.5(b).

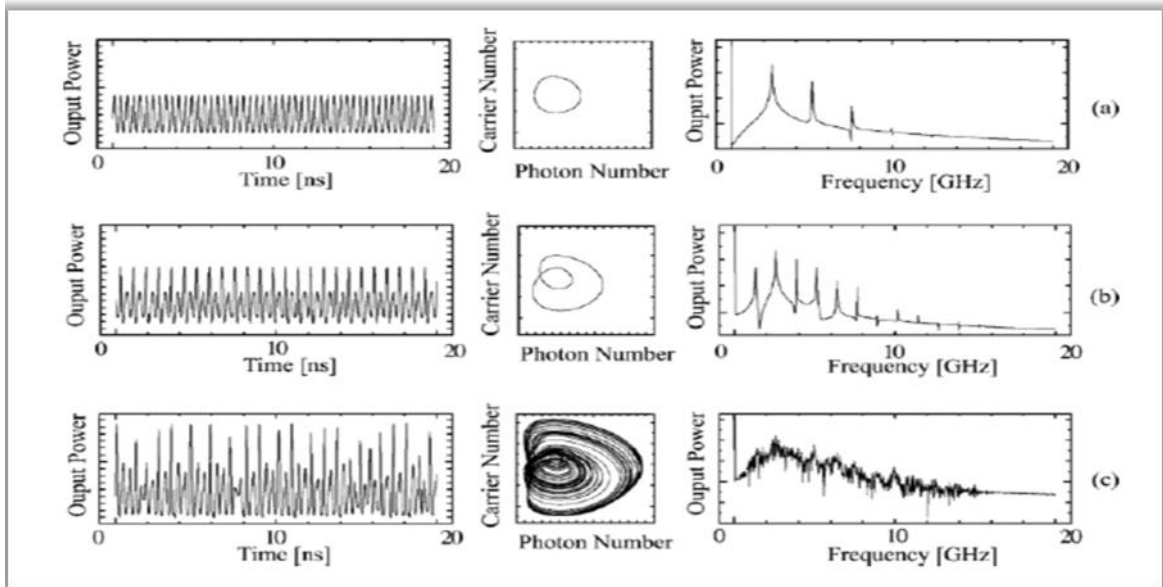


Figure:(1.5) numerically calculated time series (left row), attractors (middle row), and power spectra (right row) for different feedback ratios (Ohtsubo, 2008).

The chaotic attractor behaves in a rather different way from fixed state or periodic oscillations. At chaotic oscillations, the state goes around points within the closed compact space in the attractor; it never visits the same point in the space. The trajectory crosses in the attractor in figure 1.5(c). The chaotic trajectory goes around in a multi-dimensional space and never crosses in such a space. A chaotic attractor is quite different from other periodic oscillations and looks very strange. Therefore, it is sometimes called a strange attractor.

1.4 Chaos Analysis Tools

The properties of optical chaos can be illustrated by many parameters. So we can show these parameters as:

1.4.1 The Bursting

Bursting is a dynamic state where a neuron repeatedly fires discrete groups or bursts of spikes. Each such burst is followed by a period of quiescence before the next burst occurs. A burst of two spikes is called double, of three- spikes –triplet, four- quadruplet, etc (Szucs, et al., 2003). Burst mode is thought to be useful for signaling important events and routing information in the brain. In general, there are two types of bursting, firstly Input-driven bursting, where strong excitatory inputs produce a rapid activation and burst of action potentials, secondly Intrinsic bursting, where voltage-gated ion channels intrinsic to the neuron convert brief suprathreshold inputs into long-lasting bursts of action potential output.

Some types of neurons are able to respond to current input by emitting an all- or non-burst response. This burst usually consists of a short phase of repeated action potentials, at a frequency of up to 350 Hz. This is followed by a prolonged refractory period. In contrast, neurons that fire tonically respond with action potentials at a rate proportional to the input current.

Most mathematical models of bursting can be written in the singularly perturbed form as:

$$\begin{aligned}\dot{x} &= f(x, y) && \text{(fast spiking)} \\ \dot{y} &= \mu g(x, y) && \text{(slow modulation)..... (1.3)}\end{aligned}$$

Where x is the fast variable, a vector that simulates fast spiking of the neuron and y is the slow variable, a vector that modulates spiking activity. A topological classification of busters relies on the bifurcations of the fast subsystem (variable x) when the slow subsystem (variable y) is treated as a parameter. The subiculum is an example of a brain region where the rapid

transition between bursting and single-spiking is important for routing information out of the hippocampus.

Some definitions could be taken into account to study the neural spiking signals, like interspike (intra-burst), interburst, quiescent periods and active phase, as shown in figure (1.6).

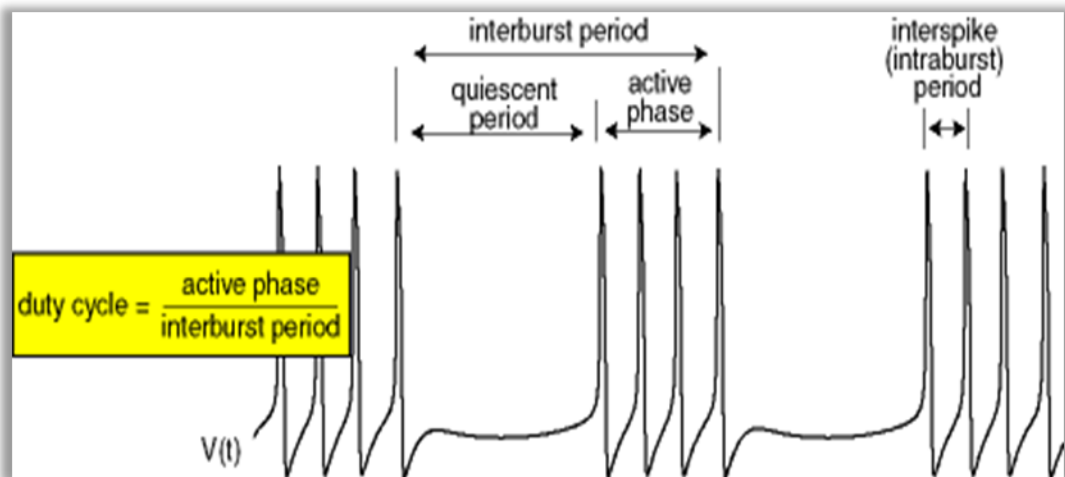


Figure: (1.6) the neural burst signal showing the duty cycle, active phase and interspike, interburst, quiescent periods (Szucs, et al., 2003).

1.4.2 Attractor in Phase Space

The onset of deterministic chaos in a dynamical system requires a three dimensional phase space, which for some parameter values can provide one positive Liapunov exponent.

We recall that a three dynamical system is characterized by three coupled first order differential equations as:

$$\dot{x}_i = f(x_i, x_j, x_k), \text{ with } \dots i \neq j \neq k = 1, 2, 3 \dots \dots \dots (1.4)$$

If the system is dissipative the sum of the Liapunov exponents' λ_i is negative; this can be satisfied by the following sets of λ_i signs $(-,-,-)$; $(-, -, 0)$; $(-, 0, 0)$; $(-, 0, +)$. The first set has contraction in all three directions, thus yielding a fixed point attractor. The second set yields a limit cycle (stable orbit in the direction of the zero Liapunov exponents), the third one a torus (composition of two limit cycles with different periods). Eventually the fourth one (with the obvious constraint that the positive exponent be smaller than the absolute value of the negative one, order to satisfy the dissipativity condition) has a "strange" attractor, with a direction along which any initial small difference is expanded to a sizable value. This sensitive dependence on the initial condition amounts to losing information in course of time and has been called "deterministic chaos" the rate of information loss is called K after the Russian mathematician Kolmogorov.

Dissipative dynamical systems are characterized by the presence of some sort of internal "friction" that tends to contract phase space volume elements. Contraction in phase- space allows such systems to approach a subset of the phase- space called an attractor as the elapsed time grows large. Attractors therefore describe the long-term behavior of a dynamical system. Steady state or (equilibrium) behavior corresponds to fixed- point attractors, in which all trajectories starting from the appropriate basin- of- attraction eventually converge onto a single point. For linear dissipative dynamical systems, fixed point attractors are the only possible type of attractor. Nonlinear systems, on the other hand, harbor a much richer spectrum of attractor types. For example, in addition to fixed-points, there may be exist periodic attractors such as limit cycles. There is also an

intriguing class of chaotic attractors called strange attractors that have a complicated geometric structure (Keizer, 1988).

1.4.3 Bifurcation Diagram

In mathematics, particularly in dynamical systems, a bifurcation diagram shows the possible long-term values (equilibrium/fixed points or periodic orbits) of a system as a function of a bifurcation parameter in the system. It is usual to represent stable solutions with a solid line and unstable solutions with a dotted line. The bifurcation is a period-doubling, a change from an N -point attractor to a $2N$ -point attractor, which occurs when the control parameter is changed. A bifurcation Diagram is a visual summary of the succession of period-doubling produced as r increases. The next figure shows the bifurcation diagram of the logistic map, r along the x -axis. For each value of r the system is first allowed to settle down and then the successive values of x are plotted for a few hundred iterations (Clayton,

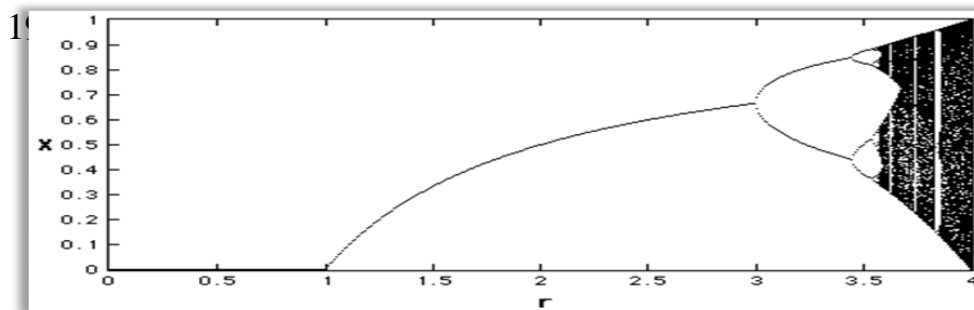


Figure:(1.7) Shows the bifurcation Diagram of the logistic map, r along the x -axis between 0 and 4 (Clayton, 1997).

We see that for r less than one, all the points are plotted at zero. Zero is the one point attractor for r less than one. For r between 1 and 3, we still have one-point attractors, but the 'attracted' value of x increases as r increases, at least to $r=3$. Bifurcations occur at $r=3$, $r=3.45$, 3.54 , 3.564 , 3.569 (approximately), etc., until just beyond 3.57 , where the system is chaotic.

However, the system is not chaotic for all values of r greater than 3.57. Let's zoom in a bit as in figure 1.8 below.

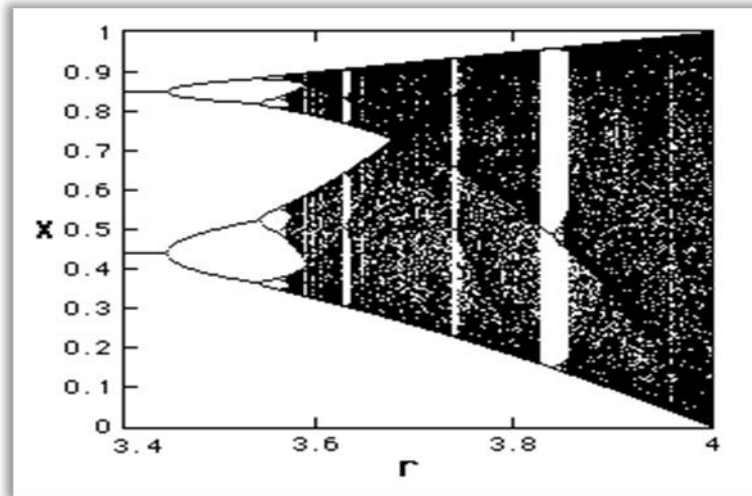


Figure: (1.8) Shows the bifurcation Diagram of the logistic map, r along the x -axis between 3.4 and 4 (Clayton, 1997).

Notice that at several values of r , greater than 3.57, a small number of x values are visited. These regions produce the 'white space' in the diagram. Look closely at $r = 3.83$ and you will see a three-point attractor. In fact, between 3.57 and 4 there is a rich interleaving of chaos and order. A small change in r can make a stable system chaotic, and vice versa (Clayton, 1997).

The bifurcation sequence chaos of a semiconductor laser (SL) subject to delayed incoherent feedback was examined experimentally and numerically by Saucedo Solorio, Sukow, Hicks and Gavrielides; (Solorio, et al., 2002). While a bifurcation diagram for a SL with external optical feedback (OPB) was studied by Pieroux and Mandel (Pieroux, and Mandel, 2003).

There are many different bifurcations: saddle-node, Hopf, period doubling (flip), torus... (Rontani, and Citrin, 2005, Iooss, Ropert, and Stora, 1983).

The saddle- node bifurcation is the basic mechanism by which fixed points are created and destroyed, as a parameter is varied. For example, the

system $\dot{x} = r + x^2$, where (r) is a parameter, there are two fixed points, one stable and one unstable, as shown in figure 1.9.

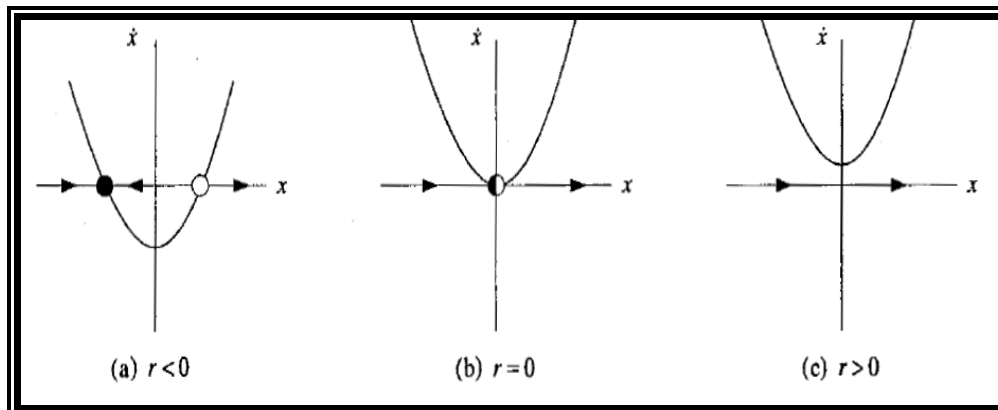


Figure: (1.9) Saddle-node bifurcation as r varied (Strogatz, 1994).

As $r < 0$, the parabola moves up and the two fixed points move toward each other. When $r = 0$, the fixed points coalesce into a half-stable fixed point at $x = 0$, the bifurcation occurred here. At $r > 0$, this type of fixed point vanishes and there are no fixed points at all.

1.5 Time Series

Time series is a set of measures of behavior over time (Clayton, (1997)).

1.6 Fast Fourier Transformation (FFT)

The Fast Fourier Transformation is an older linear tool for examining time series transforms the time domain into a frequency domain, and examines the series for periodicity. The analysis produces a power spectrum and the degree to which each frequency contributes to the series (Clayton, (1997)). If the series is periodic, then the resulting power spectrum reveals peak power at the driving frequency.

1.7 The Feedback in Dynamic Systems

A dynamical system is a system whose behavior changes over time, often in response to external stimulation or forcing. The term feedback refers to a situation in which two (or more) dynamical systems are connected together such that each system influences the other and their dynamics are thus strongly coupled. Simple causal reasoning about a feedback system is difficult because the first system influences the second and the second system influences the first, leading to a circular argument (Aström, and Murray, 2008). This makes reasoning based on cause and effect tricky, and it is necessary to analyze the system as a whole. A consequence of this is that the behavior of feedback systems is often counterintuitive, and it is therefore necessary to resort to formal methods to understand them. Figure 1.10 illustrates in block diagram form the idea of feedback.

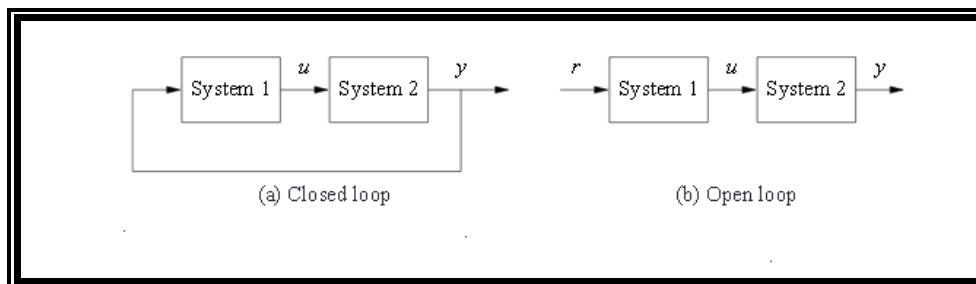


Figure: (1.10) block diagram form the idea of feedback (Aström, and Murray, 2008).

In the close loop system the output of the first system is used as the input of the second system, and the output of the second system becomes the input of the first system, creating a closed loop system and in the open loop system the interconnection between the second system and the first system is removed, and the system is said to be open loop (Aström, and Murray, 2008).

1.8 Chaos Generation in Semiconductor Laser System

All semiconductor lasers show chaotic behavior for additional perturbations such as optical feedback, optoelectronic feedback and external optical injection. And these three ways are the techniques for the generation of optical chaos in semiconductor laser. We introduce each one of them in the following subsections.

1.8.1 Laser Diode with Optical Injection

The process of optical injection is illustrated in Fig. 1.11. A single frequency signal from a master source, generally a tunable laser, is injected into the active region of the slave laser diode. The master laser is optically isolated from the slave laser (typically by a polarization dependent optical isolator) (Argyris, et al. 2005, Lawrence, 2000). Similar to optical feedback, such optical injection has a variety of effects on the operating characteristics of the slave laser. It can induce various dynamic instabilities and chaotic behavior, locks the two lasers together in phase and frequency (injection locking), excite the relaxation oscillation frequency of the slave laser, or produce phase conjugation through four-wave-mixing.

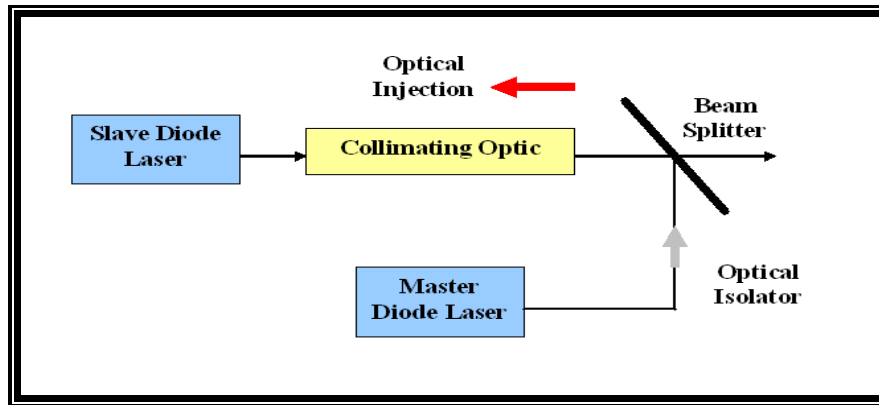


Figure: 1.11 Schematic diagram of laser diode with optical injection from another laser source (Lawrence, 2000).

1.8.2 Laser Diode with Optical Feedback

Optical feedback is introduced into a diode laser by returning some portion of the optical output back into the device. This is shown schematically in Fig.1.12. There exist two types of all-optical feedback. One is the conventional mirror optical feedback (CMOF), where the laser output is coupled into the laser internal cavity by the CMOF and the laser phase changes with the delayed feedback time. Therefore, the dynamic behaviors of laser depend on the precision positioning of the conventional mirror. The other is the phase conjugate optical feedback (PCOF), which is considerably different from the CMOF. Compared with the CMOF, the PCOF can compensate feedback phase shift. Furthermore, semiconductor laser subject to PCOF can display richer chaotic dynamics or higher dimension chaos, and the dynamics do not depend on an accurately positioning of the phase-conjugate mirror (PCM) (Lawrence, 2000).

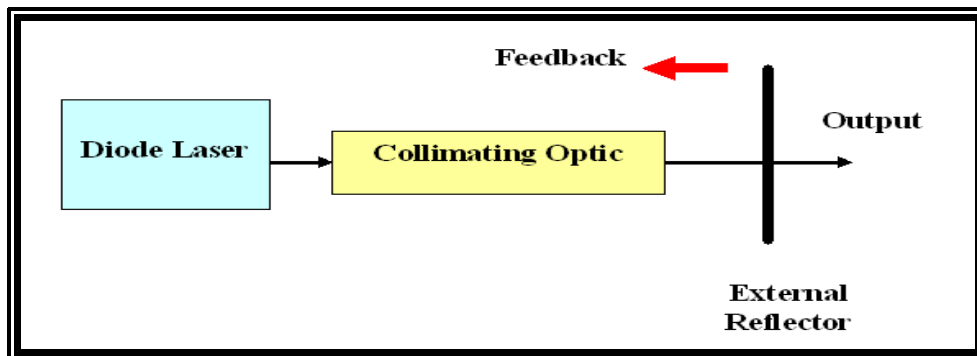


Figure: 1.12 Schematic diagram of laser diode with optical feedback (Lawrence, 2000).

1.8.3 Laser Diode with Optoelectronic Feedback

Semiconductor laser with delayed optoelectronic feedback is schematically shown in Fig. 1.13. In this configuration, a combination of photo detector and amplifier is used to convert the optical output of the laser into an electrical signal that is fed back to the laser by adding it to the injection current (Liu, Chen, and Tang, 2001). Because the photo detector responds only to the intensity of the laser output, the phase of the laser field is not part of the dynamics of this system.

In optoelectronic feedback, chaotic pulses may be generating by positive or negative feedback. Positive optoelectronic feedback is different from negative optoelectronic feedback in the mechanism that drives the nonlinear dynamics of a semiconductor laser. In the case of negative optoelectronic feedback, the feedback current is deducted from the bias current.

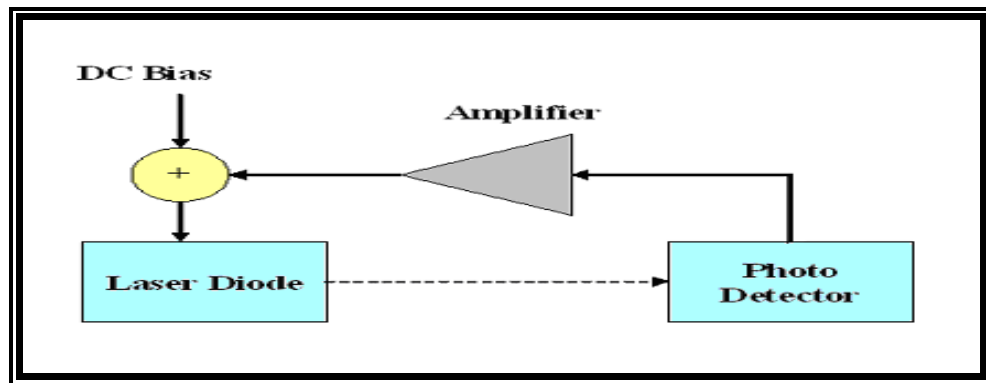


Fig. 1.13 Schematic diagram of laser diode with delayed optoelectronic feedback (Liu, Chen, and Tang, 2001).

This negative feedback current sharpens and extracts the first spike of the relaxation oscillation in the laser. In the case of positive optoelectronic feedback, however, the feedback current is added to the bias current. This positive feedback current tends to drive the laser into pulsing because of the mechanism of gain switching (Tang, and Liu, (2001).

Positive optoelectronic feedback has long been used to generate periodic short laser pulses. The repetition rate of the pulses is found to be an integral multiple of the inverse of the feedback-loop delay time that is closest to the relaxation resonance frequency of the laser.

1.9 Diode Lasers

The semiconductor lasers are unique when compared to other types of lasers. They are very small, they operate with relatively low power input, and they are very efficient. They also operate in a different way in that they require the merging of two different materials and the laser action occurs in the interface between those two materials. One of the materials has an excess of electrons (n-type) and the other material (p-type) has a deficit of electrons or an excess of holes (missing – electrons). When a forward bias voltage is placed across this junction the electrons are forced into the

region from the n-type material and holes are forced into junction from the p-type material. These electrons with a negative charge and the holes with a positive charge are attracted to each other, and when they "collide" they neutralize each other and in the process emit recombination radiation. The electrons in the n-type material exist (at normal operating temperatures) as a higher energy (conduction band) than the holes (valence band). This energy difference is designated as the band gap of the material, the amount of energy that is released when the recombination radioactive process occurs. Different material combinations have different band gaps and thus emit different wavelengths of light (Silfvast, 2004).

1.10 Fiber Optic Transceiver

The fiber optic transceiver includes both a transmitter and receiver in the same components; they are arranged in parallel so that they can operate with each others. Both the receiver and transmitter have their own circuits so that they can handle transmission in both directions as it shown in

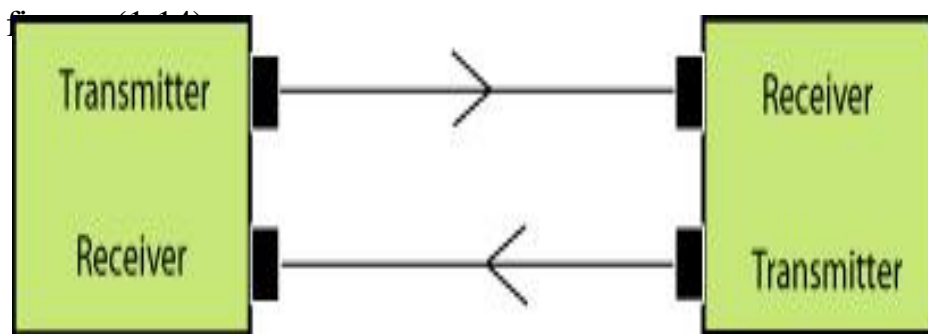


Figure: (1.14) Fiber optic transceiver block diagram (Fiber Optic Association 1999- 2013).

Fiber optic transceivers can interface with two types of cables: single mode and multimode. The first type is an optical fiber that allows only one

mode to propagate; this fiber has a very small transmission at extremely high bandwidth and allows very long transmission distance. Multimode describes a fiber optic cable which supports the propagation of multiple modes; it may have a typically core diameter of 50 to 100 μ m with a refractive index that is graded or stepped. Multimode fiber allows the use of inexpensive light emitting diodes (LEDs) as light sources; the connector and coupling is less critical than with signal mode fiber. Distance alignment transmission and transmission ion bandwidth are less than with single fiber due to dispersion. Some fiber optic transceivers can be used for both single mode and multimode cables.

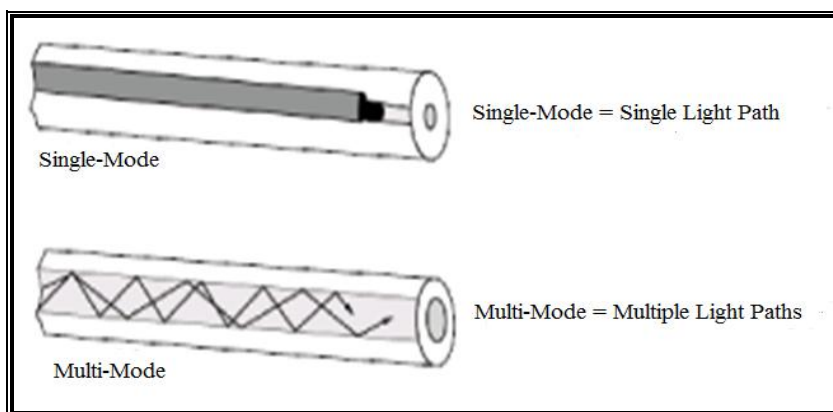


Figure: (1.15) Single mode vs. Multimode fiber (Fiber Optic Association 1999-2013).

1.10.1 Fiber Optic Transmitters

Fiber optic transmitters convert electrical signals (current, voltage) into optical signals; and then inject them into light- conducting cable. They use light emitting diodes (LEDs) or laser diodes as their optical source; and they designed for use with either single mode or multimode fibers.

Fiber optic transmitters consist of an interface circuits, a source drive circuit and an optical source. The interface circuit drives electrical signals; the source drive circuit converts them to optical signals and triggers the LEDs or laser diode then sends the light signals to fiber optic cable; where they travel to their destination

1.10.2 The Receivers' Information

The receivers contain some type of fast photo detector, normally a photo diode, and suitable high speed electronics for amplifying the weak signal, and extracting the digital or may be analog data. For high data rates circuit for electronic dispersion must be included; the main function of the receiver is to decode data as its original source. It's no secret that fiber optics is the way to go for data and voice communication. Fiber optics is that thin glass wires that carry data by form of light. A transmitter creates and codes light pulses which are sent down by means of an optical fiber. As the signal degrades regenerators amplify the signal again and transmission is completed (Ravindranadh, and Rao, 2013).

1.11 Thesis Layout

This research work organized into four chapters, chapter one is an introductory chapter, which describes the basic concepts of nonlinear dynamics systems; chaos and the description of the feedback types are given. Noise, coherence and stochastic resonance phenomena, their mechanism and their applications are described briefly in chapter two, the chapter three is discussed the experimental part, chapter four included the experiments results, discussion, the conclusion of this research work and the future research suggestions.

CHAPTER TWO

Noise, Coherence and Stochastic Resonance

2.1 Introduction

In common use, the word noise means any unwanted sound. But technically, noise is unwanted electrical or electromagnetic energy that degrades the quality of signals and data (Dhobale, Boldhan, and Burange, 2013). Noise occurs in digital and analog systems, and can affect files and communications.

Normally in hard-wired circuits the noise is of little or no consequence, but in wireless systems it's a more significant problem. In general, noise originating from outside the system is inversely proportional to the frequency, and directly proportional to the wavelength. At a low frequency such as 300 kHz, atmospheric and electrical noise are much more severe than at a high frequency like 300megahertz. Noise generated inside wireless receivers, known as internal noise, is less dependent on frequency.

Engineers are more concerned about internal noise at high frequencies than at low frequencies, because the less external noise there is, the more significant the internal noise becomes.

Communications engineers are constantly striving to develop better ways to deal with noise. The traditional method has been to minimize the signal bandwidth to the greatest possible extent. The less spectrum space a signal occupies, the less noise is passed through the receiving circuitry. However, reducing the bandwidth limits the maximum speed of the data that can be delivered. Another, more recently developed scheme for

minimizing the effects of noise is called digital signal processing. Using processing fiber optics, a technology far less susceptible to noise, is another approach. The types of noise are thermal noise, shot noise, flicker noise, burst noise, transit time noise and avalanche noise (Devi, and Shinde, 2013).

2.2 Types of Noise

There are several types of noise sources in electrical circuits like:-

1. Thermal or (Johnson – Nyquist) Noise.
2. Shot Noise.
3. 1/f Noise (Also called Flicker or Pink noise).
4. White Noise.
5. Burst Noise.

However, we discuss some of important noise sources here.

2.2.1 Thermal Noise

Thermal noise goes under a number of names including Johnson-Nyquist noise, Johnson noise, or Nyquist noise (Ian, 1998). This noise gained its various names because it was first detected and measured by John B. Johnson in 1926, and later explained by Harry Nyquist - both were Bell Labs and working together. Thermal noise is a random fluctuation in voltage caused by the random motion of charge carriers in any conducting medium at a temperature above absolute zero. This electrical noise is generated as a result of thermal agitation of the charge carriers which are typically electrons within an electrical conductor. Thermal noise actually occurs regardless of the applied voltage because the charge carriers vibrate as a result of the temperature. This vibration is dependent upon the temperature - the higher the temperature, the higher the agitation and hence

the thermal noise level. Thermal noise, like other forms of noise is random in nature. . Fig: 2.1 pictured the thermal noise.

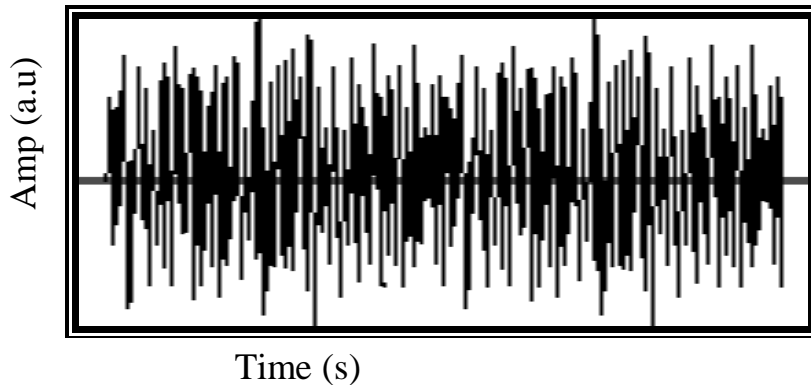


Fig: 2.1 Thermal noise signal as seen on an oscilloscope trace (Ian, 1998).

Thermal noise appears regardless of the quality of component used in circuits. The noise level is dependent only upon the temperature and the value of the resistance. Therefore the only ways to reduce the thermal noise content are to reduce the temperature of operation, or reduce the value of the resistors in the circuit.

Other forms of noise may also be present; therefore the choice of the resistor type may play a part in determining the overall noise level as the different types of noise will add together. In addition to this, thermal noise is only generated by the real part of any impedance, i.e. the resistance. The imaginary part does not generate noise. The following equations are used for calculating Johnson noise (Romero, 1998, Ott, 1988).

$$\text{Johnson noise power } P_J (\text{rms}) = (kT\Delta f) \quad (2.1)$$

$$\text{Johnson noise voltage } V_J (\text{rms}) = (4 kTR\Delta f) \quad (2.2)$$

$$\text{Johnson noise current } I_J(\text{rms}) = (4kT\Delta f/R) \quad (2.3)$$

Where k is the Boltzmann constant (1.38×10^{-23} Joules/Kelvin), T is Temperature in Kelvin ($K= 273+^{\circ}\text{Celsius}$), R is Resistance in Ohms, Δf is Bandwidth in Hz in which the noise is observed.

Johnson noise is typically modeled as a noiseless resistor either in series with a noise voltage source or in parallel with a noise current source (Sobering, 1999). Note that stray shunt capacitance limits noise voltage since as R increases, Δf decreases. Johnson noise models shows in figure

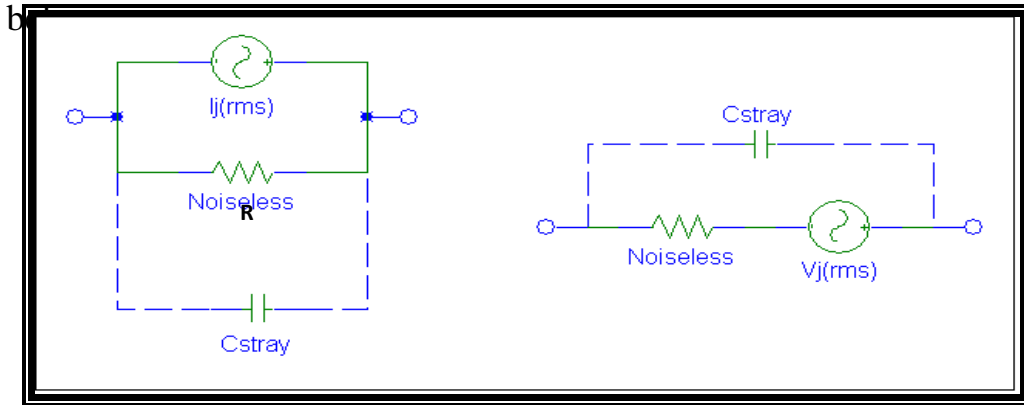


Figure :(2.2) Johnson noise models (Sobering, 1999).

2.2.2 Shot Noise

Shot noise results from the flow of current across a potential barrier, it is a statistical effect of the random emission of electrons (and holes) or the production of photoelectrons. It is found in vacuum tubes, transistors, and diodes. Shot noise is given by (Michael, 2005).

$$I_{\text{sh}}(\text{rms}) = (2 q I_{\text{DC}} \Delta f)^{1/2} \quad (2.4)$$

Where q represents electron charge (1.6×10^{-19} coulombs), I_{DC} denotes average current dc current (A) and B denotes noise bandwidth (HZ).

Like Thermal noise, Shot noise is proportional to $\sqrt{\Delta f}$ meaning that there is constant noise power per Hz bandwidth, i.e. it is white noise.

2.2.3 Low Frequency Noise

Low frequency noise (or excess noise) has a $1/f$ (where f denotes the frequency) power spectrum. This type of noise occurs only when current flows through a device in contradistinction to Johnson noise that does not

require an applied voltage. In the case of $1/f$ noise, the charged particles move under the applied field and randomly encounter a scattering center or trap. The change in motion of the particle results in noise. The low frequency noise has a number of alternative names including excess noise, current noise, pink noise and semiconductor noise. This noise is in addition to the Johnson noise already present.

Also referred to as contact noise (when found in detectors), excess noise (resistors), or flicker noise (vacuum tubes) (Ott, 1988). $1/f$ noise is not well understood. It increases without limit as frequency decreases. It has been measured at frequencies as low as $6 \times 10^{-5} \text{Hz}$ ($\approx 5 \text{cycles/day}$). If an amplifier is $1/f$ noise limited, measurement accuracy cannot be improved by increasing the length of the measurement (averaging). In detectors, it is related to the quality of Ohmic contacts and surface states. It also appears in composition-type resistors, carbon microphones, switch and relay contacts, transistors and diodes and therefore all amplifiers. For a photovoltaic detector flicker noise current calculated by (Michael, 2005).

$$i_{\text{rms}} = k(i_b^\alpha \Delta f/f_\beta)^{1/2} \quad (2.5)$$

where k is proportionality constant, i_b is the current through the detector, $\alpha =$ typically 2 and $\beta =$ typically ~ 1 .

$1/f$ noise is often ignored in noise computations where the system bandwidths are high; it is the dominant noise source in low-frequency applications (e.g. seismic detectors)

2.2.4 White Noise

White Noise is the noise that has constant magnitude of power over frequency, and its frequency spectrum is flat. Examples of White Noise are Thermal Noise, and Shot Noise.

2.3 Coherence Resonance (CR) in Chaotic Systems

A resonance is defined as the presence of a maximum in the response of the system as a function of some control parameter (for instance, the frequency of the external signal). It is nowadays well established that, in some cases, the response of a nonlinear dynamical system to an external forcing can be enhanced by the presence of noise (fluctuations) (Palenzuela, et al. 2001). Coherence resonance (CR) is the phenomenon due to noise bridging different configurations of a bistable or multistable system. It refers to coherent motion stimulated by noise on the intrinsic dynamics of the system without the presence of an external periodic forcing (Arecchi, and Meucci, 2009). As noise is applied to a chaotic system, a train of an intensity spikes separated by an erratic inter-spike interval (ISI) appeared, and when the (ISI) distribution is smoothed out, by means of adding an external periodical force the CR phenomena is observed.

The Inter-Spike Intervals is a model for studying the properties of irregular spiking homoclinic chaos and the dynamics of spiking and bursting in a neuron model. ISI mean measures time between consecutive spikes. The discrete distribution of ISI decays exponentially and have peaks located at all natural (Bodova, 2009).

The coherence resonance CR occurs in an excitable system driven by noise. The output of such a system can become quite regular when an appropriate amount of noise is added. This phenomenon was initially called as SR without external periodic excitation or autonomous SR, and was named as CR later (Jin, and Haiyan, 2007).

Huxley *et al.* found that the coherence of an excitable system could become maximal near saddle equilibrium by choosing a moderate amount of noise excitation. Pikovsky and Kurths investigated the effects of noise on the Fitz Hugh–Nagumo system and found CR by adding a limited amount of noise. Pradines *et al.* showed that the CR relied on the coexistence of both slow and fast motions (Jin, and Haiyan, 2007).

The Fitz Hugh–Nagumo (FHN) model is a simple but representative example of excitable systems that occur in different fields of application ranging from kinetics of chemical reactions and solid-state physics to biological processes.

The equations of motion for this system are: (Pikovsky, and Kurths, 1997).

$$\varepsilon \frac{dX}{dt} = X - \frac{X^3}{3} - Y \quad (2.6)$$

$$\frac{dY}{dt} = X + a + D\xi(t)$$

(2.7)

Here ε , a , are parameters and D governs the amplitude of the noisy external force ξ .

According to the previous facts we notice that the noise has a constructive role which represented in the coherence and stochastic resonance phenomena.

The mechanism of CR characterizes by two time scales:-

Activation time t_a (residence time in the ground state) which mean the time between end of one spike and the beginning of another in the time series of the signal spectrum; this time t_a strong dependence on noise intensity and follows Kramer's formula as in the equation bellow (Pikovsky, and Kurths, 1997).

$$t_a \propto \text{Exp} [\Delta V/D^2] \quad (2.8)$$

Where D denotes the noise intensity and Δv denotes the variation coefficient.

The second time is the excursion time t_e (time needed to reach the ground state after the excitation event) or decay time of unstable state.

The sum of these two times called the inter-spike interval t_p . Figure 2.3 depicted that.

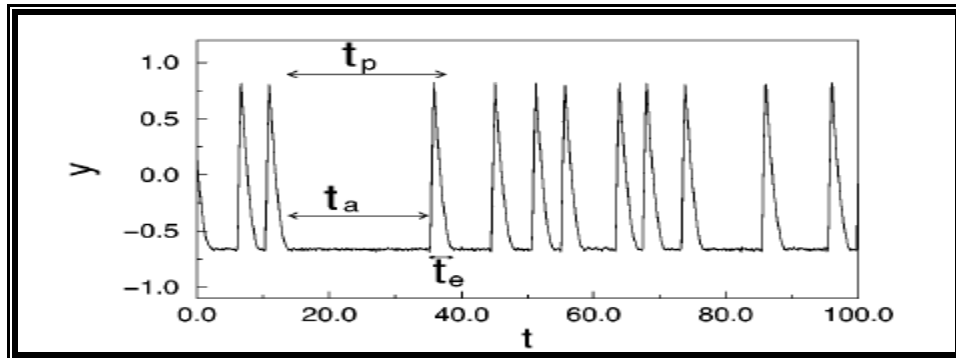


Figure:(2.3) the dynamics of the Fitz Hugh–Nagumo system [Eqs. (6), (7)] for $a = 1.05$, $\varepsilon = 0.01$, $D = 0.02$ (Pikovsky, and Kurths, 1997).

The first experimental observation of CR in an optical system has been recently made in a semiconductor laser with optical feedback (Giacomelli, et al., 2000). In that case, noise was added to the driving current of the laser, giving rise to a pulsed behavior in the system, in the form of the well known low-frequency fluctuations (LFF). The regularity of the dropout series initially increased with increasing noise level, and peaked for an optimal amount of noise. In our work we used same previous regime but with optoelectronics feedback to identification the CR phenomenon.

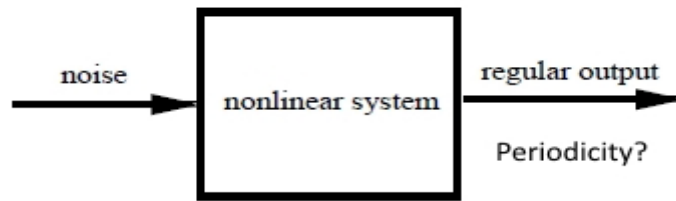


Figure 2.4: Coherence Resonance principle: proper noise intensity optimizes the periodicity of the system output.

CR may be calculated by different ways like Power Spectral Density (PSD), Auto Correlation Function (ACF), but we used the Co-efficient of variation (V_N) or Normalized variation which is well common, as in equation below:

$$V_N = \frac{\sqrt{\langle T^2 \rangle - \langle T \rangle^2}}{\langle T \rangle}$$

(2.9)

Here T is the inter-spike time interval.

2.4 Stochastic Resonance (SR) in Chaotic Systems

Over the last two decades, stochastic resonance has continuously attracted considerable attention. The term is given to a phenomenon that is manifest in nonlinear systems whereby generally feeble input information (such as a weak signal) can be amplified and optimized by the assistance of noise. The effect requires three basic ingredients: firstly an energetic activation barrier or, more generally, a form of threshold; secondly a weak coherent input (such as a periodic signal); finally a source of noise that is inherent in the system, or that adds to the coherent input. Given these features, the response of the system undergoes resonance-like behavior as a function of the noise level; hence the name stochastic resonance. The underlying mechanism is fairly simple and robust. As a consequence, stochastic

resonance has been observed in a large variety of systems, including bistable ring lasers, semiconductor devices, chemical reactions, and mechanoreceptor cells in the tail fan of a crayfish (Gammaiton, et al., 1998).

By other words the stochastic resonance (SR) is a phenomenon where a signal that is normally too weak to be detected by a sensor, can be boosted by adding white noise to the signal, which contains a wide spectrum of frequencies. The frequencies in the white noise corresponding to the original signal's frequencies will resonate with each other, amplifying the original signal while not amplifying the rest of the white noise (thereby increasing the signal-to-noise ratio SNR which makes the original signal more prominent). Further, the added white noise can be enough to be detectable by the sensor, which can then filter it out to effectively detect the original, previously undetectable signal (Moss, Ward, and Sannita, 2004).

2.4.1 The Single - to - Noise Ratio (SNR)

In a noise added system it is convenient to define the signal to noise ratio as follows:

$$SNR = S_p(\nu) / S_n(\nu)$$

(2.10) Where $S_p(\nu)$ indicates the peak of the output signal spectrum, calculated the frequency ν of the periodic forcing signal and $S_n(\nu)$ indicates the output signal spectrum at the same frequency ν but without the periodic forcing signal (Ando, and Graziani, 2000).

2.4.2 The Mechanism of the Stochastic Resonance

When linear coupling takes place between signal and noise, usually the noise acts as a nuisance degrading the signal. In contrast, when certain

types of nonlinear interaction take place between signal and noise, there may exist possibility of cooperation between the signal and the noise. The presence of the noise then becomes beneficial to the signal, up to a point where an increase of the noise may improve the performance for transmitting or detecting the signal. Stochastic resonance (SR) designates this type of nonlinear effect whereby the noise can benefit to the signal. This paradoxical effect was first introduced some twenty years ago in the domain of climate dynamics, as an explanation for the regular recurrences of ice ages. Since this origin, SR has been largely developed and extended to a broad variety of domains. Today, it is possible to synthesize the various forms observed for SR by means of the scheme of Fig: 2.5

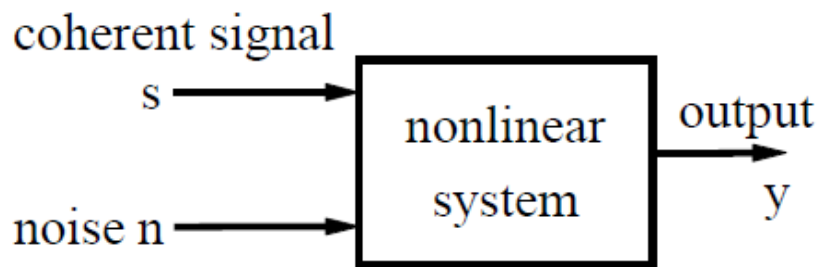


Figure:(2.5) A general scheme for stochastic resonance(Chapeau and Blondeau, 2000).

The previous figure 2.4 consists in the possibility of increasing the similarity between the information-carrying or coherent input signal s and the output signal y by means of an increase of the level of the noise D . Stochastic resonance, as illustrated by the figure 2.5 above involves four essential elements:

- (i) An information-carrying or coherent signal; s : it can be deterministic, periodic or none, or random.
- (ii) A noise D , whose statistical properties can be of various kinds (white or colored, Gaussian or none . . .).

(iii) A transmission system, which generally is nonlinear, receiving s and η as inputs under the influence of which it produces the output signal; y .

(iv) A performance or efficacy measure, which quantifies some similarity between the output y and the coherent input s (it may be a signal-to-noise ratio, a correlation coefficient, Shannon mutual information . . .) (Hafeez, and Blondeau, 2000).

We can also calculate SR by the co-efficient of variation as in equation 2.9 (periodic SR) or by the Cross Correlation Co-efficient (A periodic SR) see the equation 2.11

$$C_o = \langle (X_1 - \langle X_1 \rangle_t)(X_2 - \langle X_2 \rangle_t) \rangle_t \quad (2.11)$$

Where: X_1 is the time series of a periodic input signal, X_2 is the time series of noise induced output signal and $\langle \rangle_t$ is time average.

SR has been found in ring lasers, in systems with electronic paramagnetic resonance, in tunnel diodes, in experiments with Brownian particles, in chemical systems, in visual perception, in the food detection system of paddlefish and in human cognition.

2.4.3 A simple Model of Stochastic Resonance

We will look at a one dimensional system, a particle in one space dimension, described by a Langevin equation with a potential of two minima together and a time-periodic forcing it shows as in following figure:

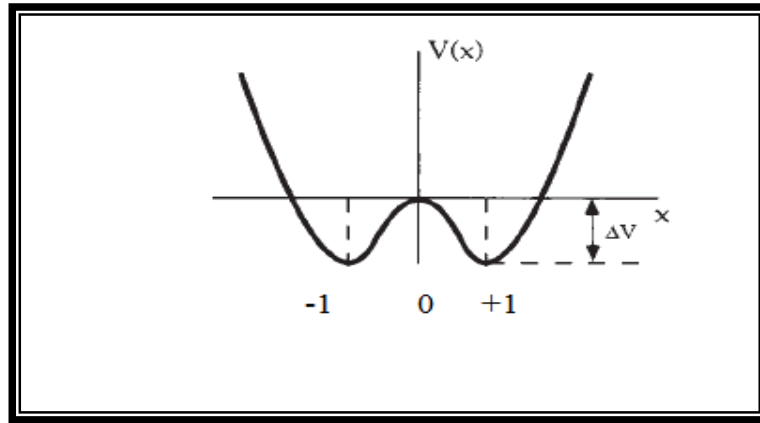


Figure:(2.6) sketch of the double- well the minima are located at $x \pm 1$ (Gammaiton, et al. 1998).

The time independent potential find as flowing (Hilbom, 2004).

$$V(x) = \frac{1}{4} x^2 - \frac{1}{2} x \quad (2.12)$$

The periodic forcing, or (signal) is: $- A \sin(t) x$

Sticking to our example, this is the periodic change in air pressure due to an approaching bird. We have introduced a constant A , the amplitude of the periodic forcing.

The time dependent effective potential of the system is:

$$V(x,t) = \frac{1}{4} x^2 - \frac{1}{2} x^2 - A \sin(t) x \quad (2.13)$$

Including noise leads to this Langevin equation:

$$dX = -V(X_t, t)dt + \sqrt{2D}dw_t = (X_t - X_t^3) + A \sin(t)dt + \sqrt{2D}dw_t \quad (2.14)$$

The potential has two local minima at $x = \pm 1$.

In the context of the example of the introduction, the case $x < 0$ is that a neuron is not active and $x > 0$ is the case that a neuron is active (active in the sense that the neuron distributes an electrical signal along its axon).

The potential wall between the minima has a height of $\frac{1}{2}$. If the amplitude of the periodic forcing is below this value, and there is no noise ($D = 0$), the system won't be able to do a transition from one minimum to the other. Therefore, if we observe the system, i.e. the position of our particle as a function of time $x(t)$, we won't see any signal. According to our example, the neurons will stay in one state, like not active, and the poor cricket will have no chance to detect what is approaching.

If we increase D to a very high value, the particle will jump arbitrarily between the two minima, and again we won't see any signal. Heuristically it seems clear that there should be a value for D such that the signal to noise ratio is optimal: In this case the influence of white noise increases the signal to noise ratio to a level such that the signal is observable (Hilbom, 2004).

The influence of noise with different amplitudes on the periodic forcing in a nonlinear dynamic regime illustrated below in figure 2.7.

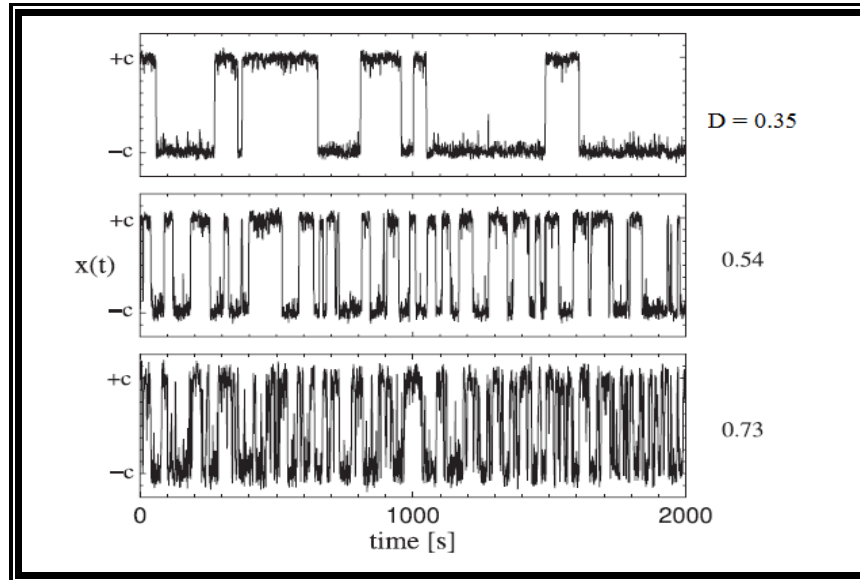


Figure : (2.7) Single realizations of $x(t)$ in the periodically modulated double well potential, for three different values of the noise strength, D (Wellens, Shatokhin, and Buchleitner, 2004).

The noise-induced synchronization of $x(t)$ with the periodic input signal is poor for the lowest noise level (rare random transitions), optimal for intermediate noise strength (almost regular transitions) and again poor for strong noise (too frequent transitions per cycle of the periodic drive) (Wellens, Shatokhin, and Buchleitner, 2004).

2.4.4 Applications of Stochastic and Coherence Resonance

The stochastic and coherence phenomena have much application in many fields; here we mentioned some of them as examples.

Hugh a mound of applications in SR throughout a large spectrum of fields (about 1000 or more) published since 1981 like:

- Optics
- Biology
- Neurology
- Psychophysics

2.4.4.1 Neuroscience

Stochastic resonance has been observed in the neural tissue of the sensory systems of several organisms (Kosko, and Bart, 2006). Computationally, neurons exhibit SR because of non-linearities in their processing. SR has yet to be fully explained in biological systems, but neural synchrony in the brain (specifically in the gamma wave frequency) has been suggested as a possible neural mechanism for SR by researchers who have investigated the perception of subconscious visual sensation (Ward, et al., 2006).

2.4.4.2 Medicine

SR-based techniques have been used to create a novel class of medical devices for enhancing sensory and motor functions such as vibrating insoles especially for the elderly, or patients with diabetic neuropathy or stroke (Gammaitoni, et al., 1998).

Stochastic Resonance has found noteworthy application in the field of image processing.

2.4.4.3 Signal analysis

A related phenomenon is dithering applied to analog signals before analog-to-digital conversion (Gammaitoni, 1995). Stochastic resonance can be used to measure transmittance amplitudes below an instrument's detection limit. If Gaussian noise is added to a subthreshold signal, then it can be brought into a detectable region. After detection, the noise is removed. A fourfold improvement in the detection limit can be obtained (Palonpon, et al. 1998).

As the SR the CR phenomenon has applications in many fields:

- Neuronal and biological systems
- Chemical models
- Electronic circuits
- Semiconductors laser

2.5 Literature Review

In the last two decades the world has witnessed an enormous growth of results achieved in other sciences - especially chemistry and biology - based on applying methods of stochastic processes. One reason for this stochastic boom may be that the realization that noise plays a constructive rather than the expected deteriorating role has spread to communities beyond physics. Besides their aesthetic appeal these noise-induced, noise-supported or noise-enhanced effects sometimes offer an explanation for so far open problems (information transmission in the nervous system and information processing in the brain, processes at the cell level, enzymatic reactions, etc.).

They may also pave the way to novel technological applications (noise-enhanced reaction rates, noise-induced transport and separation on the nanoscale, and noise-supported phenomena in excitable systems.), where noise can play an eminent role as phenomena of structure formation. Spirals, fronts, kinks, interfaces, domains, growing surfaces, etc., usually modeled theoretically by physicists, are important for many real phenomena in physics, chemistry and biology, e.g. current filaments in semiconductors, catalytic reactions on surfaces, and the complex dynamics of the heart, of the brain, or of ecosystems. It is an amusing fact of history that the theory of stochastic processes was initiated in 1828 by Robert Browns observation of the irregular motion of pollen grains suspended in

water. As a botanist - which is more akin to a biologist than to a physicist - he was inclined to explain his observation by endowing the pollen grains with a vital force, the molecules of life. Actually, his biologically inspired idea has been revived recently by physicists opening the research field of active Brownian particles. Later, Brown convinced himself - and others - those tiny particles of inorganic substances were also subjected to the same motion. As a consequence, Brownian motion soon drifted from biology to physics where Einstein (1905) and Smoluchowski (1906) published theories, which proved to be a first major breakthrough. From this perspective it is interesting to see that stochastic processes and Brownian motion have made their way from biology to physics to chemistry and back to biology. In about 1980 R. Benzi, G. Parisi, A. Sutera, A. Vulpiani and C. Nicolis introduced a mathematical approach to qualitative explanation of the phenomenon of glacial cycles (Benzi, et al., 1981, Nicolis, 1982). The modern methods of acquiring and interpreting climate records indicate at least seven major climate changes in the last 700,000 years. These changes occurred with the periodicity of about 100,000 years and are characterised by a substantial variation of the average Earth's temperature of about 10K. In 1983, experimental studies by S. Fauve and F. Heslot showed the phenomenon of stochastic resonance in a simple electronic device (Fauve, and Heslot, 1983). The Schmitt trigger investigated by them is a very simple and well-known electronic circuit, characterized by a two state output and a hysteretic loop, extensively studied by physicists. The Schmitt trigger provides another interpretation to the phenomenon of stochastic resonance. A system displaying stochastic resonance can be considered as a sort of random amplifier. The weak periodic signal which cannot be detected in the absence of noise can be successfully recovered if the system (the Schmitt trigger) is appropriately tuned. In other words, the weak underlying

periodicity is exhibited at appropriately chosen non-zero levels of noise, and gets lost if noise is either too small or too large.

It was not before 1988 when stochastic resonance was used again in experiments performed on an optical system known as bidirectional ring laser (McNamara, Wiesenfeld, Roy, 1988). Thereafter, the effect of stochastic resonance has been found in a variety of physical systems and studied by a variety of physical measures of quality of tuning: passive optical bistable systems (Dykman, et al., 1991), in experiments with magnetoelastic ribbons (Spano, Fogle, and Ditto, 1992), in superconducting quantum interference devices (Hibbs, et al. 1995). In 1993 J. K. Douglass, L. Wilkens, E. Pantazelou, and F. Moss, were the first group to demonstrate SR in sensory neurons. They (surgically) isolated single mechanoreceptor neurons from crayfish tailfins, along with the associated nerve roots and abdominal ganglions, and immersed them in crayfish saline. The neuron was mounted vertically on an electromagnetic motion transducer activated by the sum of a signal and a random noise. In crayfish, mechanoreceptors are responsible for transducing the movements of small hairs into signals (spikes) that propagate along the nerve. The group showed noise-induced signal enhancement in ten out of the eleven mechanoreceptor cells tested. They concluded that they had demonstrated that biological systems had the ability to use SR and they raised the question of whether organisms had evolved to exploit SR (Douglass, et al., 1993). In 1995 Collins, J., Chow, C. and Imho, T., demonstrate that a FitzHugh-Nagumo network of neurons has the capacity to detect a sub-threshold multi-frequency signal using a noise source with known characteristics. The result is really interesting because, in the system investigated, it separates the persistence of SR conditions from the noise amplitude. This is an extension of the aperiodic SR (ASR) phenomenon,

observed in certain systems in the presence of aperiodic forcing signals, to complex systems (Collins, Chow, and Imho, 1995). In 1998 L. Gammaitoni, P. Haggis, P. Jung, and F. Marchesoni, have been described of the mechanism regulating the transitions of a stochastic system forced by a sub-threshold periodic component. More specifically, it describes the effect of oscillations of a quadratic potential forced by a periodic component. On account of the symmetry of the system the two wells of the potential alternately take on two different levels. The two Kramers rates, to which different meaning and significance can be attributed are associated with the two levels (Gammaitoni, L. et al. 1998). In 1999 Russell, D. F., Wilkens, L.A. and Moss, F., study of paddle fish feeding and showed that the paddle fish fed from a wider area when an optimal amount of noise was added to the system, compared to both the control, when no noise was added, and the case when high (above optimal) noise was added and suggest that paddle fish have evolved to use the noise produced by the sum of signals from individual Daphnia in a dense swarm to highlight the presence of a single Daphnia emitting its own signal (Russell, Wilkens, and Moss, F. 1999). In 2000, Jia, Y., Yu, S. N. and Li, J. R. studied the SR phenomenon in a bistable system under the simultaneous action of multiplicative and additive noises using the adiabatic limit method (Jia, Yu, and Li, 2000). In 2003 Luo, X., and Zhu, S. studied SR in a bistable system driven by two different kinds of colored noises and found that there seemed to be a transition between one peak and two peaks in the curve of the SNR when either the noise correlation time or the coupling strength between the additive noise and the multiplicative noise was increased (Luo, and Zhu, 2003). In 2004, M. Avila, F. Jhon, de S. Cavalcante, L. D. Hugo, and R. Leite, have achieved the CR in a semiconductor laser without external noise, experimental, in the low frequency fluctuations of a chaotic

diode laser with optical feedback, and numerically using the Lang-Kobayashi equations for a single solitary mode laser, without noise terms and proved that the fast deterministic dynamics plays the role of an effective exciting noise (Avila, M. et al. 2004). Also SR phenomenon studied by J. M. Buldu, J. Garcia-Ojalvo, M. C. Torrent, J. M. Sancho, C. R. Mirasso, and D. R. Chialvo, in semiconductor lasers with optical feedback which operate in the low-frequency fluctuation (LFF) regime and concluded that the output intensity of the laser shows an irregular pulsated behavior in the form of sudden intensity dropouts and these resonances are caused by the help of external colored noise introduced through the pumping current of the laser and reported new type of stochastic resonance, where a nonlinear system shows a resonance at a frequency not present neither at its internal time scales nor at any external perturbation, this phenomenon, known as ghost resonance (Buldu, et al. 2004). In 2007, Cao, L. and Wu, D. J., studied the SR of periodically driven linear system with multiplicative white noise and periodically modulated additive white noise (Cao, and Wu, 2007). In 2008, P. S. Burada, G. Schmid, D. Reguera, M. H. Vainstein, J. M. Rubi, and P. Haggi, presented a novel scheme for the appearance of SR when the dynamics of a Brownian particle took place in a confined medium (Burada et al.2007). In 2009, Du, L. C. and Mei, D. C., investigated the SR phenomenon of a periodically driven time-delayed linear system with multiplicative white noise and periodically modulated additive white noise (Du, and Mei, 2009). Wu, D., Zhu, S. and Luo, X. studied coupled bistable oscillators with different sources of diversity, and found that the resonance was reduced, and even disappeared, as the correlation length between the diversity increased (Wu, Zhu, and Luo, X. 2009). Stochastic Resonance and Coherence Resonance phenomena in experiments using CO₂ lasers reported by F.T. Arecchi and

R. Meucci, and they were discussed a quasi-isotropic laser where noise induces switching between two intensity components with mutually orthogonal polarization, concluded SR and CR in dynamical systems as lasers, does not correspond to coexistence of stable fixed points as in the original formulation of SR and CR, but is rather due to different phase space trajectories associated with a saddle focus singularity. Applying the method of unified colored noise approximation (Arecchi, F. and Meucci, R. 2009). In 2010, L. Zhao, X. Q. Luo, D. Wu, S. Q. Zhu, and J. H. Gu, investigated the phenomenon of entropic SR in a two-dimensional confined system driven by a transverse periodic force when colored fluctuation was included in the system (Zhao, et al. 2010). In 2013 Y. Xu, J. Li, J. Feng, H. Zhang, W. Xu, and J. Duan, investigated the SR phenomenon induced by Levy noise in a second-order and under-damped bistable system, observed that the noise intensity and amplitude of external signal affect the systems output power spectrum that reaches a peak value at a constant frequency and the increase of the amplitude or noise intensity in a certain range further enhances this peak value, which illustrates that the appropriate noise intensity and amplitude lead to the optimal occurrence of the SR phenomenon (Xu, et al. 2013).

CHAPTER THREE

The Experimental Part

3.1 Introduction

This chapter consists of the description of the components of the experimental setup that used in this work, and it concentrated on the transition of the electrical signal because it represents the main purpose of the project.

Also this chapter showed the method that followed to achieving chaotic signals by using semiconductor laser in nonlinear dynamical systems and how these chaotic signals affected by noise to obtain coherence and stochastic resonance.

3.2 The Equipment

We used a number of devices or equipments in this experimental work such as:-

DC power supply, an optical transmitter, an optical receiver, an optical fiber, two cathode ray oscilloscopes, Ac-coupled nonlinear optoelectronic feedback (electro-optical feedback), function generator, variable amplifier, noise generator (White noise) source, an optical and electrical cables.

3.2.1 DC Power Supply

The DC power supply of 0 -30 volts/ 5 amperes is used as electrical source to derived a signal with value of 5.2 volts through an optical transmitter into injector with power input (5- 6)volts. The characteristics of this DC power supply showed in the table below.

Table (3.1) Shows Characteristics of the DC Power Supply 30V/5A

Item	Data
Device name	DC power supply 30V/5A
Voltage range	0- 30V
Current range	0- 5A
Line voltage	200-240V/AC
Mains frequency	50H-60Hz
Company	MCH-China
Efficiency	+85%
Ripple and noise	20 mA
Size	7(w)x16(h)x22(D)
Weight	1.35kg
Load regulation	10-100%
Line regulation	120-240V/AC
In put current at 220V/AC,full load	0.44A

DC power supply 30V/5A is pictured in figure 3.1 as it exhibited below.



Figure: (3.1) shows the photograph of the DC power supply 30V/5A.

3.2.2 Optical Transmitter

In this experiment a Philip Harris optical transmitter, which has electronic circuits to convert electrical signals (current, voltage) into optical signals in form of laser diode (LD) has been displayed in figure 3.2, it consists of:

1. Power input 5-6V
2. Monitor output
3. Modulation input 300kHz
4. Optical source with output injector of 1mm diameter fiber
5. Four capacitors, six diodes, seven resistances and one integral circuit



Figure (3.2) the schematicview of optical transmitter.

3.2.3 Optical fiber

A single mode optical fiber is used to get alignment flexibility between the laser source in the optical transmitter and the photo detector in the optical

receiver. The most important specifications of this fiber are summarized in table (3.2).

Table (3.2) the optical fiber specifications.

Item	Data
Core diameter	8-10 nm
Cladding diameter	125nm
Core material	SiO ₂
Cladding material	SiO ₂
Channel	1FC/PC=0.25
Length	3 meters
Connectors	FC/PC-ceramic
Number of connectors	1

3.2.4 Optical Receiver

The Philip Harris optical receiver was used to reconvert the optical signal to an electrical signal the pictured shape of optical receiver showed in figure 3.3 its components are:

1. Photo detector with input injector of 1mm diameter fiber
2. Two Output unit
3. Power input 5-6V.
4. Adjust output with range of 0-10 maximum gain.
5. Five capacitors, three diodes, sixteen resistances and two integral circuits.



Figure (3.3) an optical receiver.

3.2.5 Analog Oscilloscope

An oscilloscope, previously called an Oscillograph, and informally known as a scope, CRO (for cathode-ray oscilloscope), or DSO (for the more modern digital storage oscilloscope), is a type of electronic test instrument that allows observation of constantly varying signal voltages, usually as a two-dimensional plot of one or more signals as a function of time. Non-electrical signals (such as sound or vibration) can be converted to voltages and displayed. Analog oscilloscope is used in this work to observe the change of an electrical signal over time, the waveform against the scales built into the screen of the instrument, beside that we used it as amplifier. This oscilloscope was manufactured in German, by HAMEG Company, type: HM 1004-3,

power maximum is 38 watts at 240V/50Hz, AC 100-240V/50/16Hz. figure (3.4) illustrated this analog oscilloscope.

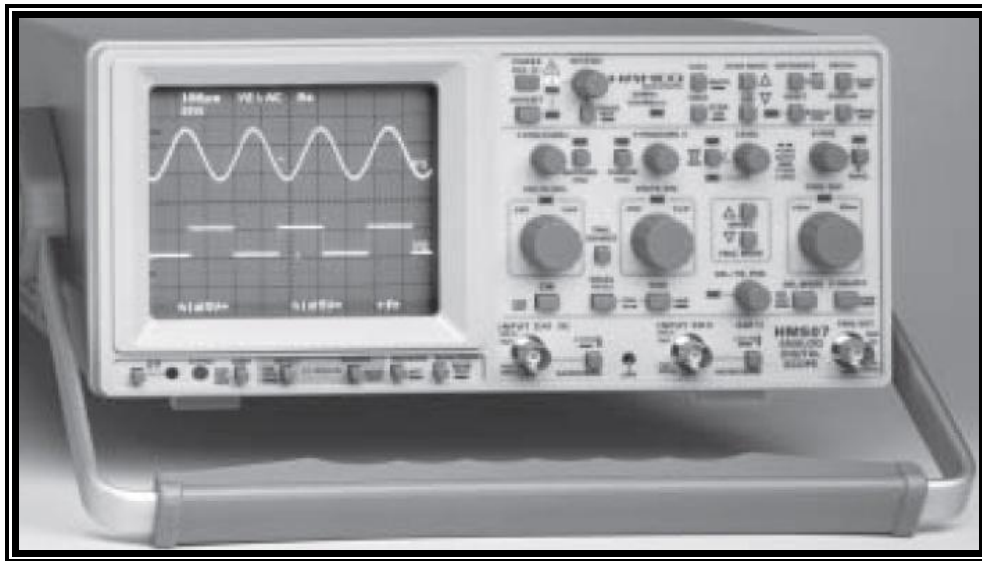


Figure: (3.4) Analog Oscilloscope HM 1004-3.

3.2.6 Digital Oscilloscope

The digital oscilloscope with memory device was used in our work to display the electrical signals that amplified by the analog amplifier and the optoelectronic feedback device to be recorded. The specifications of this oscilloscope mentioned in table (3.3).

Table (3.3) the specifications of the digital oscilloscope.

Item	Data
Device name	TDS2012c Two channel digital storage oscilloscope
Voltage range	100-120
Frequency	50-60Hz, when operate at 115V the frequency is 400Hz
Company	Tektronix
Power maximum	30 watts in both case
Serial NO.	TDS2012c Co 19798

The digital oscilloscope is pictured in figure 3.5 as it exhibited below.



Figure: (3.5) TDS2012c Two channel digital storage oscilloscope photograph.

3.2.7 Function Generator

The function generator or the waveform generator is used in this work to accurate the frequency. The function generator provides a frequency from 0.1 Hz to 100 kHz. And also we used it to form different waveforms, either a sinusoidal, triangular or square wave. Apart from being used in time processes control, a function generator can be used in the control of amplifiers. Its specifications and photograph are in table (3.4) and figure (3.6) respectively.

Table (3-4) the specification of function generation

Item	Data
Device name	Function generation
Order NO.	13652.93
Serial NO.	360500183464
Voltage	230 V
Mains frequency	50/60 Hz
Power consumption	10 VA
Maximum output voltage	$10V/R_i = 50\Omega$
Distortion at 1KHz	
Company	PHYWE - GERMAN

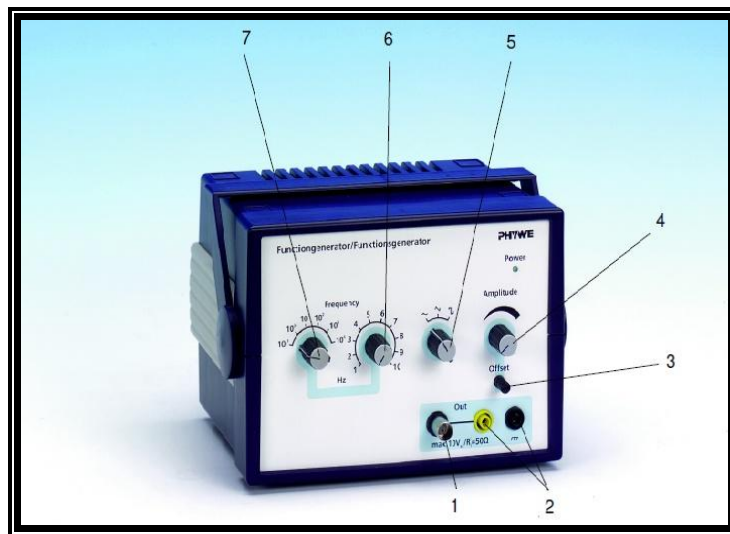


Figure (3.6) Front view of the Function generator Order NO: 13652.93

Where: 1) BNC connector 2) 4mm Output sockets 3) Offset control knob 4) Amplitude control knob 5) Signal waveform step switch 6) Coarse frequency steep switch.

3.2.8 The White Noise Generator

AWG430 200 MS/s Arbitrary Waveform Generator from Tektronix, which have zero mean, Gaussian shape, bandwidth ranging from 20 Hz to 200 KHz which has the ability to generate sine wave with the addition of white noise

With independent control of both through a single channel, this property enables us to control of sinusoidal and noise intensities on both alone.

The photograph of the white noise generator pictured as in figure 3.7



Figure (3.7) Front view of the white noise generator

3.3 The Experimental setup

One way for obtaining incoherent feedback via the injection current of the laser is the optoelectronic feedback, and it is efficient technique to externally control the spectral features of semiconductor lasers.

Many control parameters play crucial roles in generating a chaotic behavior of laser output. These parameters are laser power, injection current of the laser diode and the amplifier gain. Figures (3.7-a), (3.7-b) illustrated Schematic and photographic the experimental setup.

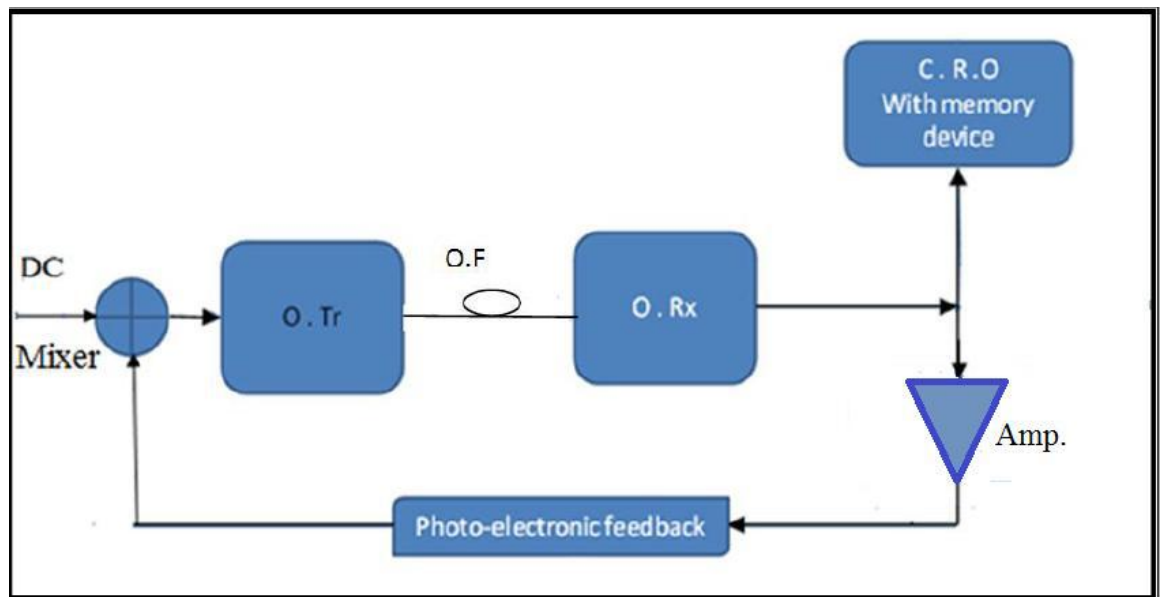


Figure (3.8-a): Schematic experimental setup for chaotic generation.

Where: DC, power supply, (O.T), optical transmitter, (O.F), optical fiber (O.R_x), optical receiver, (C.R.O), cathode ray oscilloscope.

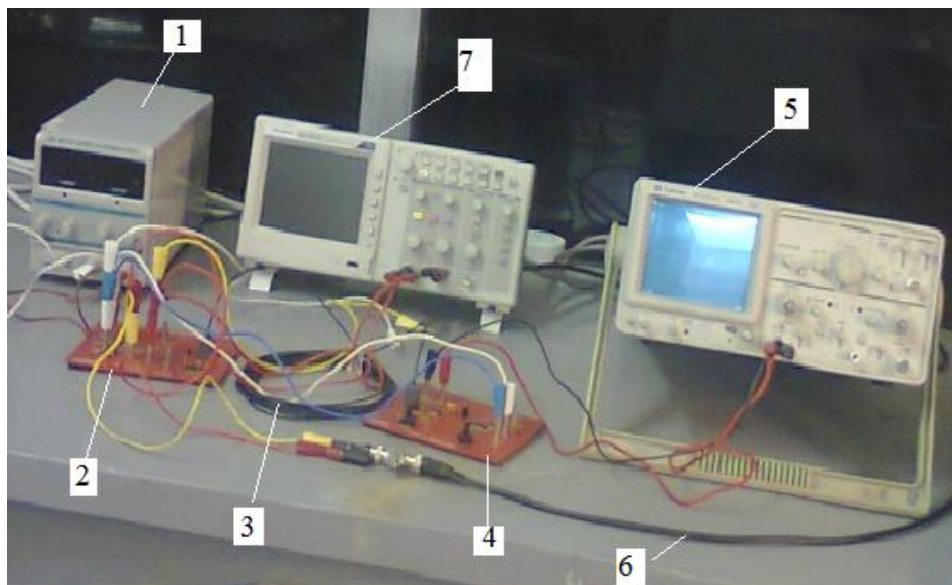


Figure (3.8-b): Photographic experimental setup for chaotic generation

Where: 1) DC power supply. 2) Optical transmitter. 3) Optical fiber. 4) Optical receiver. 5) C.R.O, used as amplifier. 6) Optoelectronic feedback. 7) C.R.O, with memory device.

3.4 The Method

The experimental setup of generating chaos signal by optoelectronic feedback was layout as in previous two figures. It contains of DC power supply, optical transmitter, optical fiber, optical receiver, two cathode ray oscilloscopes (C.R.Os) one of them has output behind and the other with memory device, and photo-electronic feedback. In this experiment we derived an electrical signal (voltage), with value of 5.2 V from the DC power supply 30V/5A, through the input injector: 5-6V on the optical transmitter.

The optical transmitter converted the voltage (electrical) signal to an optical signal and triggered the laser diode (LD), in the visible region which represented as an optical source.

The output signal (an optical signal) from the optical source was launched into an optical fiber and transmitted to fast photo detector on the optical receiver which reconverted the optical signal to an electrical signal again. Then the spectrum of the output electrical signals, observed into the oscilloscope that deals as amplifier because the signal attenuated through the optical fiber cable.

In this work the current was back injected to the power source again via the technique so called photo electronic feedback, which forced the signal to the unstable state or chaos signal, and this chaotic signal displayed on the other oscilloscope with memory device to be recorded.

After the free chaotic signal generated in dynamic system (it must be nonlinear system) by means of the optoelectronic feedback; the sinusoidal wave from the function generator device was added to accurate the frequency of the chaotic signals. To do that the frequency was adjusted at limit value as 10khz, 20khz,... and varied the voltage between 10mV, 20mV,30mV,...for each frequency value . And the same thing has done for

fixing the voltage at certain values and changed the values of the frequency. Figure below shows the addition of function generator device to the setup of chaotic signal generation.

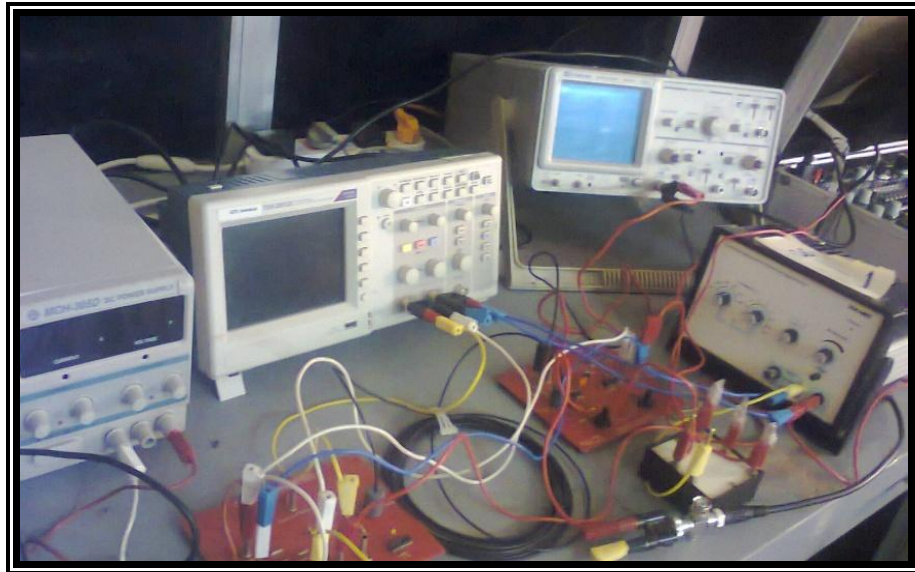


Figure (3.8-c) Experimental setup photographic with the waveform generator.

This chapter consisted of the main parts of our work, the first, is an experimental part, which include the configurations of regime under an optoelectronic feedback to getting the chaos, the second part is to apply noise to study the coherency of the chaotic laser system and also drive that chaotic system by periodic signal and noise signal to study the stochastic resonance phenomenon.

3.5 Coherence Resonance

We have a system which is operating in a homoclinic chaos regime where the output intensity consists of a chaotic sequence of spikes, and so CR refers to coherent motion stimulated by noise on the intrinsic dynamics of the system without the presence of an external periodic forcing (Wu, Zhu, and Luo, 2009). We demonstrate the effect of noise in our system to investigate the role of external noise; a Gaussian noise generator is inserted into the feedback loop. Experimentally the noise which produced by a AWG430 200 MS/s Arbitrary Waveform Generator from Tektronix, added to the bias current of the laser; the noise has Gaussian shape, bandwidth ranging from 20 Hz to 200 KHz and it's amplitude is a controllable parameter, as shown in figure 3.8.

Here, noise was added to the driving current of the laser, giving rise to a pulsed behavior in the laser output, in the form of the well known low-frequency fluctuations (LFF). The regularity of the dropout series initially increases with increasing noise level, and peaked for an optimal amount of noise.

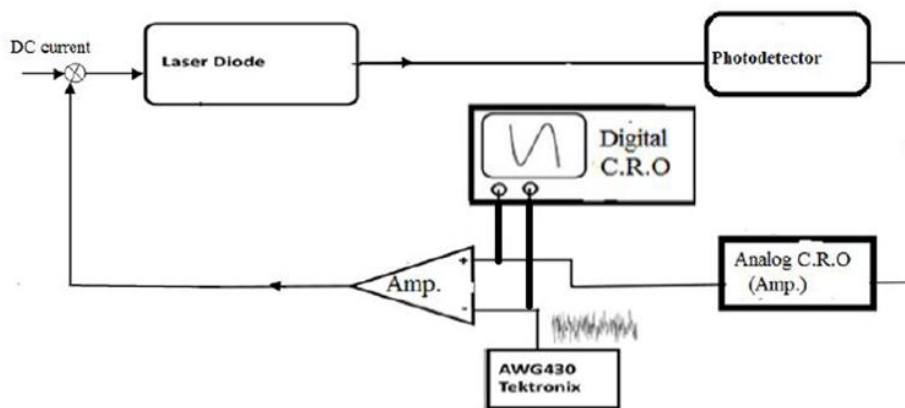


Figure 3.9: Experimental Setup of Coherency

2.6 Stochastic Resonance

In certain systems, noise may optimize the signal transfer, that is, adding a given amount of noise to the input can maximize the SNR at the output. This phenomenon is called stochastic resonance and it is one of the most exciting topics in current noise research. SR means that the output SNR is a maximum as a function of input noise intensity (Jung, and Hanggi, 1989, Locher, 2000). So SNR has the following definition.

$$\text{SNR} = P(\omega_0) / S_N(\omega_0) \quad (3.1)$$

$P(\omega_0)$ is the input signal power and $S_N(\omega_0)$ is the PSD of the noise at frequency ω_0 . The experimental setup of stochastic resonance (SR) illustrated in the following figure.

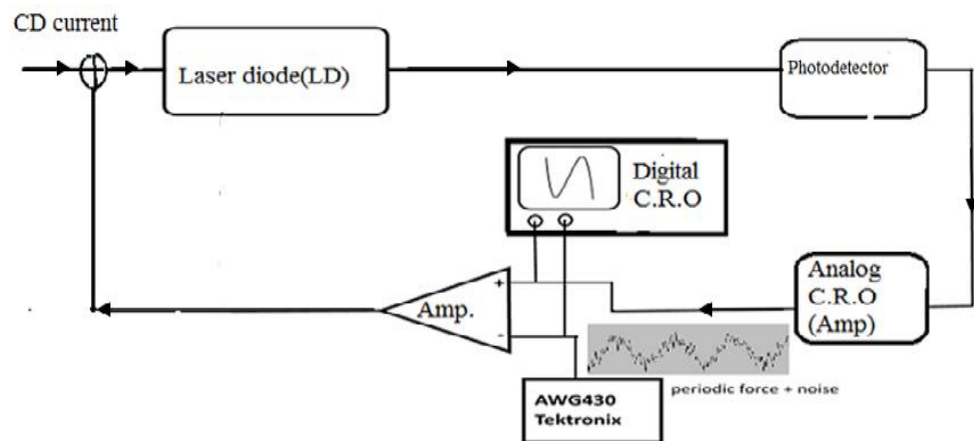


Figure 3.10: Experimental Setup of Stochastic Resonance Procedures

3.7 Dynamical model

The structure of semiconductor lasers (SL) is based on the p-n junction and the laser oscillation is realized by the emission of light due to carrier recombination between the conduction and valence bands, namely, inter-band optical transitions. This band structure of actual lasers is not modeled by a simple two-level system, but it becomes possible to use this approximation if we know that the intra-band relaxation within the medium

of the SL is fast enough of the order of 10^{-13} s compared with the carrier recombination rate of 10^{-9} s (Ohtsubo, 2013). The SL is classified into class B and therefore, the polarization term is adiabatically eliminated and the effect is simply replaced by the linear relation between the field and the polarization.

The population inversion for SLs is replaced by the carrier density N produced by electron-hole recombination. The photon number (which is equivalent to the absolute square of the field amplitude) and the carrier density are frequently used as the variables of the rate equations for SLs. However, for the general descriptions of the dynamics in SLs, we must employ the complex amplitude of the field (the amplitude and the phase of the field) instead of the photon number.

The dynamics of the photon density S and carrier density N is described by the usual single mode SL rate equations appropriately modified in order to include the ac-coupled optoelectronic feedback (Al-Naimee, et al. 2009, Al-Naimee, et al. 2010, and Ciszak, et al. 2011).

$$\dot{S} = [g(N - N_t) - \gamma_o]S \quad (3.2)$$

$$\dot{N} = \frac{I_o + f(I)}{eV} - \gamma_c N - g(N - N_t)S \quad (3.3)$$

$$\dot{I} = -\gamma_f I + \kappa \dot{S} \quad (3.4)$$

where I is the high-pass-filtered feedback current (before the nonlinear amplifier), $f_F(I) \equiv AI/(1 + s'I)$ is the feedback amplifier function, A is the amplifier gain and s' is a saturation coefficient, I_o is the bias current, e the

electron charge, V is the active layer volume, g is the differential gain, N_t is the carrier density at transparency, γ_o and γ_c are the photon damping and population relaxation rate, respectively, γ_f is the cutoff frequency of the high-pass-filter and k is a coefficient proportional to the photo-detector responsivity.

Compared with optical feedback, optoelectronic feedback is reliable and robust because the system is insensitive to optical phase variations. For this reason the phase dynamics of the optical field can be eliminated. A detailed physical model of the system should include also a series of low-pass frequency filters arising from the limited bandwidth of the photodiode, the electrical connections to the laser, parasite capacitances, and other undesirable electronic effects.

CHAPTER FOUR

Results, Discussion and Conclusions

4.1 Introduction

This chapter includes the experimental results and discussion, which related to investigation of the evidence of the spiking generation in semiconductor laser specific (laser diode) with a closed loop ac-coupled optoelectronic feedback. The effects of feedback strength and the bias current on the chaotic behavior of semiconductor laser as control parameters, have been demonstrated by means of the time series, FFT, attractor and in focus the bifurcation scheme due to the providing a complete description of the system behavior under the influence of a certain parameter.

Also in this chapter we concentrated our investigation on the experimental results that displayed the stochastic coherence (SC) or coherence resonance (CR) and stochastic resonance (CR) phenomena in the excitable nonlinear semiconductor lasers systems when they triggered by white noise in the absence or in the presence of the externally perturbations (signals) respectively.

The analysis and Origin version 8.0 Software are used to analyze the time series generated in the chaos regime. The analysis concerns the study of the attractors and the Fast Fourier transformations (FFT) of the output spectrum.

4.2 The Experimental Results

4.2.1 Optoelectronic chaotic dynamics

The motivation behind the study the chaos characteristic of our framework, recognize the parameters that make our framework a chaotic framework, then will stay unchanged when the study of the impacts of noise and modulation signal to achieve the presence of nonlinear framework as a key component for the investigation of (SR) and (CR) phenomena.

4.2.1.1 The influences of variable Bias current on the chaos state

When the optoelectronic feedback loop that illustrated in figure (2.7-a) in chapter two was closed, an output voltage proportional to laser power is observed with the screen of the digital oscilloscope and it could be recorded.

By increasing gradually the intensities of the bias current δ_0 to varied values, while keeping the feedback strength $\varepsilon = 0$, we see time series transition from a line at $\delta_0 = 0$ mA) to sinusoidal oscillations then periodic oscillations and finally to a chaotic state.

In the following section we will shows some chaotic waveforms within this Sequence and plot them. In Fig.4.1, when the bias current of (4.1mA).the time series shows a stable distinguished optical power which has a semi-sine motions as in Fig.4.1 (a).

The corresponding attractor by using an embedding technique showed in Fig.4.1 (b). And the corresponding FFT, represented through Fig.4.1(c), one main frequency is appeared with high amplitude.

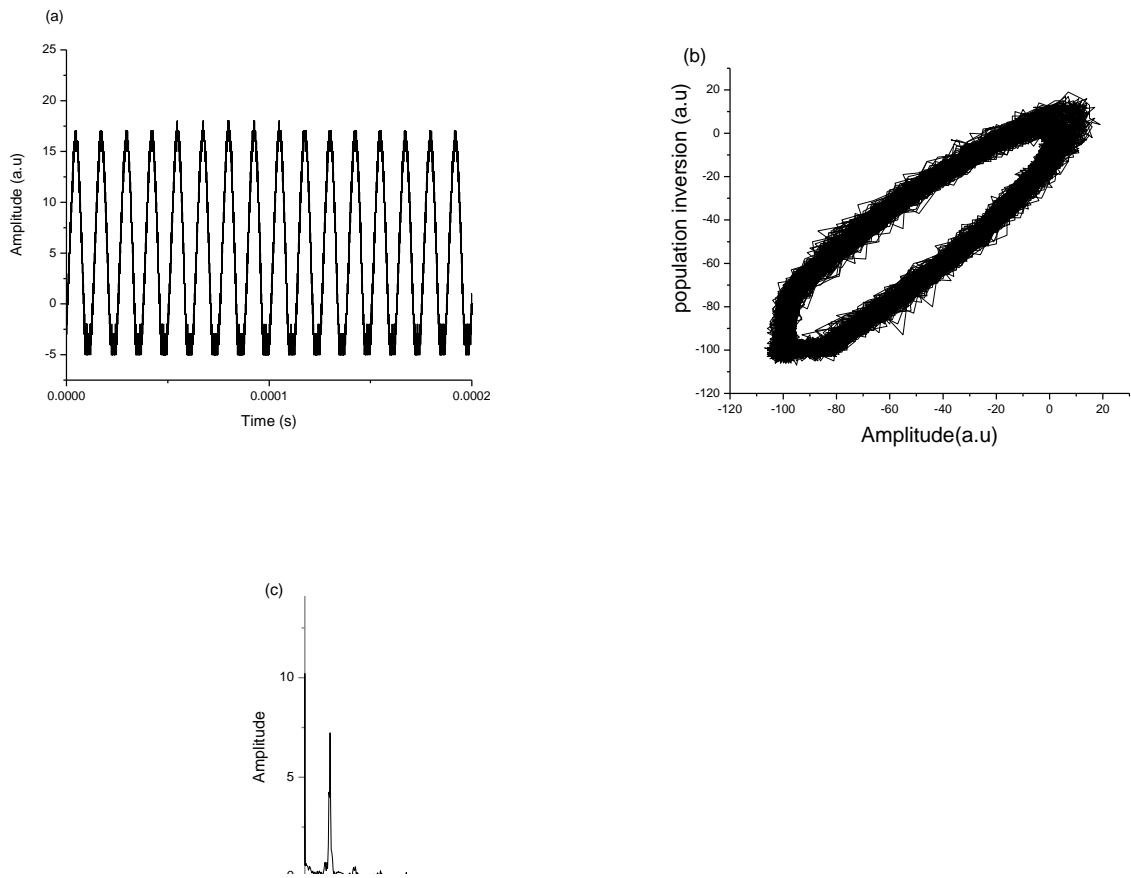


Figure 4.1: (a) Experimental time series of system at $\delta_0 = 4.1\text{mA}$, (b) the corresponding attractor,(c)the corresponding FFT.

By increasing the bias current to 5.8mA, show cases no general periodicity, where expansive intensity heartbeats are isolated by sporadic time intervals in which the framework shows small amplitude chaotic motions.

Figure 4.2 displayed that case where Fig.4.2 (a), 4.2(b) and 4.2(c) represent the time series which appear the beginning of branching in the output power spectrum, the corresponding attractor and the FFT respectively.

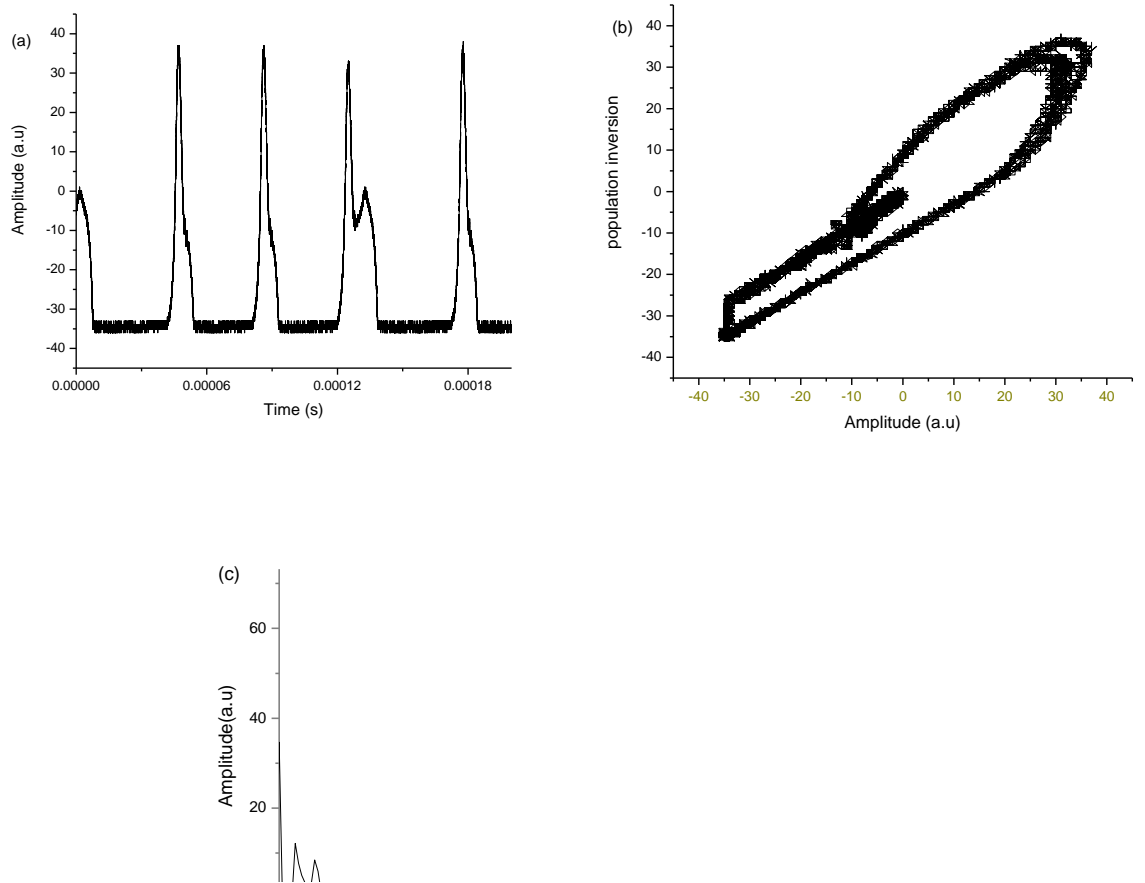


Figure 4.2: (a) Experimental time series of system at $\delta_0 = 5.8\text{mA}$, (b) the corresponding attractor, (c) the corresponding FFT.

When increasing the value of bias current to 8.2mA the irregularity of the power output laser intensity is increasing and we noticed more branching in the system dynamical sequence, as it exhibited in Fig.4.3

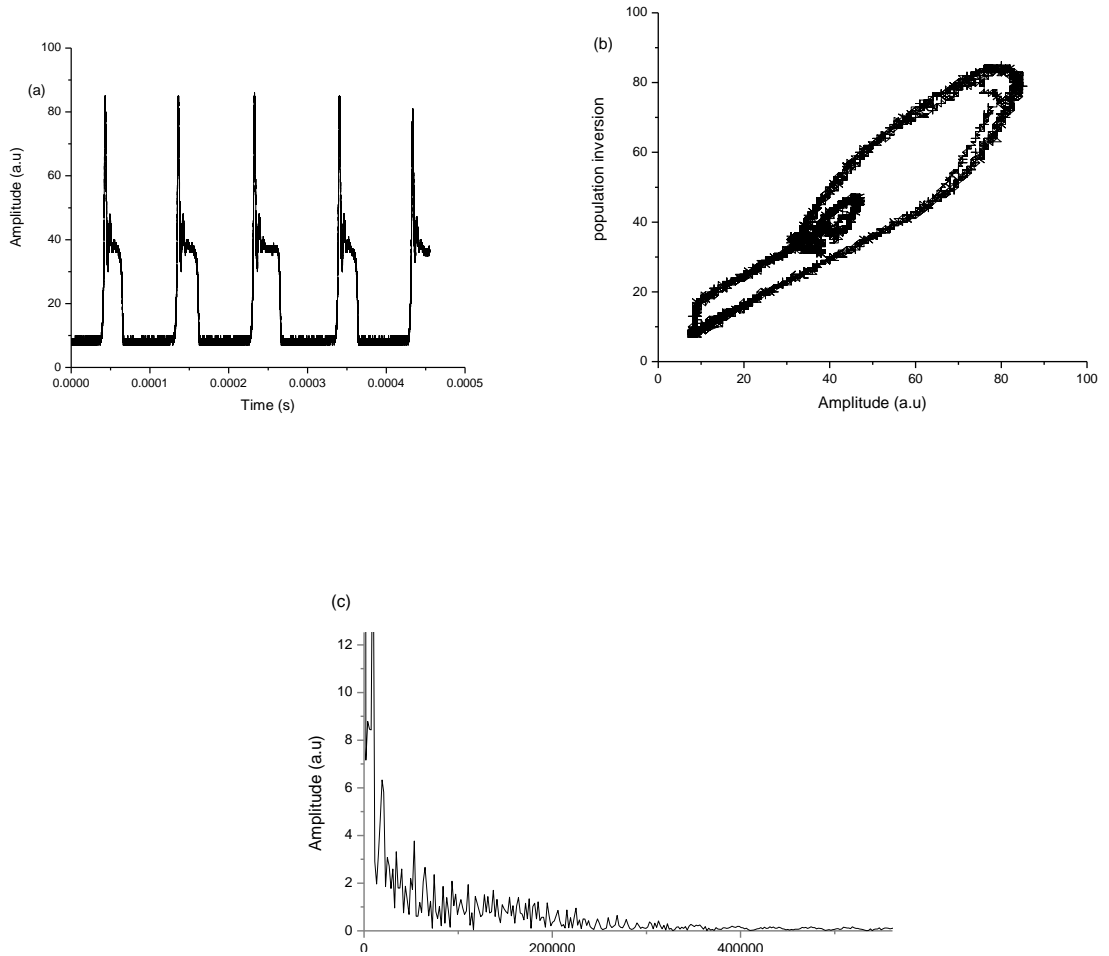


Figure 4.3: (a) Experimental time series of system at $\delta_o = 8.2\text{mA}$, (b) the corresponding attractor, (c) the corresponding FFT.

As the δ_o is more increased the dynamical behavior of the nonlinear will be chaotic, Fig. 4.4 shows that a chaotic state is developed at bias current above the previous values, and the different peaks is increased by the effect of the feedback current. We notice that the corresponding FFT shows the increasing of different frequencies of this state, the system turned to chaotic. The results showed that, when the intensity of bias current δ_o increases, the stability in the chaotic regime decreases, so the δ_o is the one of the important

parameters to generate chaos in nonlinear dynamical laser systems by optoelectronic feedback (see Fig 4.4).

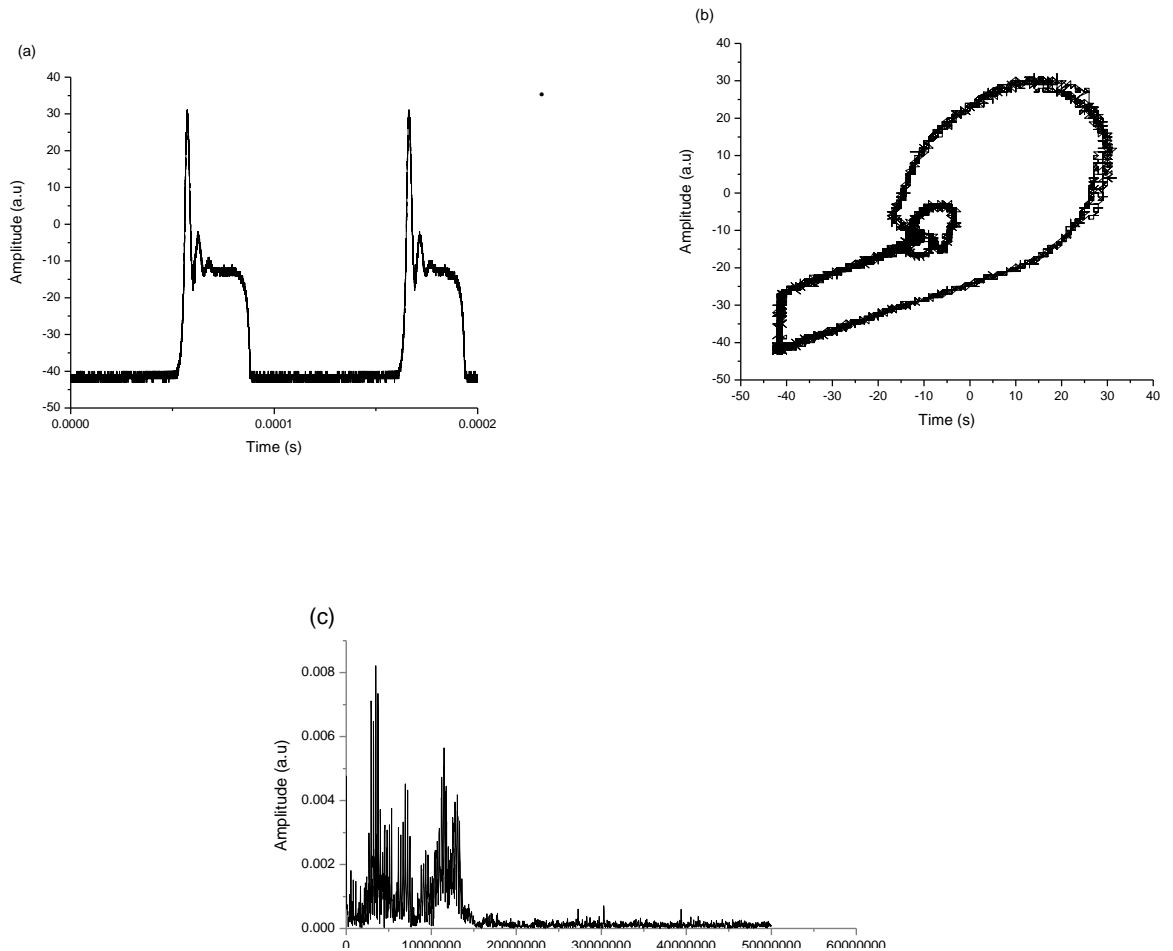


Figure 4.4: (a) Experimental time series of system when $\delta_0 = 9\text{mA}$ (b) the corresponding attractor, (c) the corresponding FFT.

The way to the chaos process in nonlinear laser systems is manifested (illustrated) clearly with a bifurcation diagram; we plot the bifurcation diagram of the peak-to-peak laser output intensity with the bias current as a control parameter as it showed in Fig: 4.5 below. From the figure one notes that the dynamical behavior of the regime is fully ruled by the bias current and it's transmitted progressively from a stable state to chaos state due to the intensity of the bias current δ_0 , where the feedback strength ε must be fixed at a constant value.

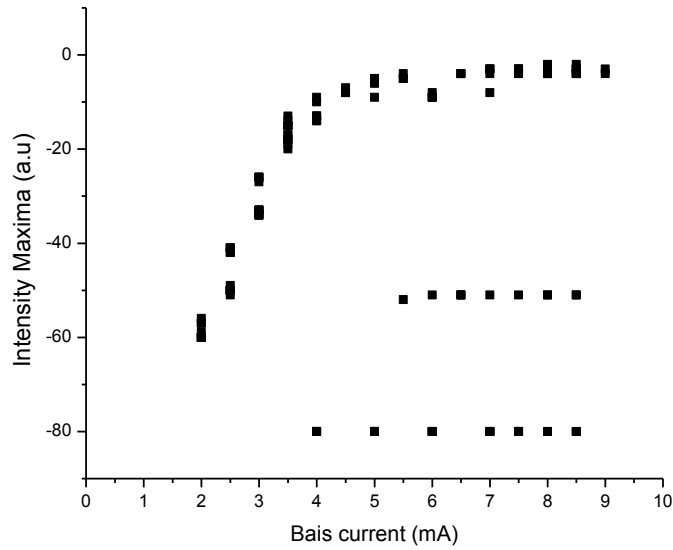


Figure 4.5: Bifurcation diagrams (maxima of photon densities vs bias current as a control parameter.)

The interpretation of the bifurcation diagram is as follows. For a given bias current, the absence of points in the diagram indicates a stable equilibrium. A few numbers of points for a given bias current corresponds to a periodic limit-cycle. Finally, a more number of points correspond to quasi periodicity or chaos.

4.2.1.2 The Influences of Variable Feedback Strength on the Chaos state

When we fixed the dc-bias laser current in constant value of 8.mA, and changing the feedback strength ε , a similar dynamical sequence as in previous section can be obtained as long as bias current is kept constant and the amplifier gain is changed. Here we used the voltage amplification factor A_v as feedback strength to study the effect of the negative optoelectronic feedback for our system with higher nonlinear gain reduction factor.

The observed intensity spectra with the increase of the feedback strength (the values of the amplification) are being shown in following figures of the time series, corresponding FFT and attractor.

Initially we have started with feedback strength value $\varepsilon = 0$, in this case the system will be at steady state and the corresponding attractor is the fixed point, that means there is no nonlinear dynamic could be seen.

When the feedback is $\varepsilon = 0.78$, the transition from steady state to semi-sine oscillations with slight difference in amplitudes are appeared on the output optical laser power as shown in figure 4.6(a).

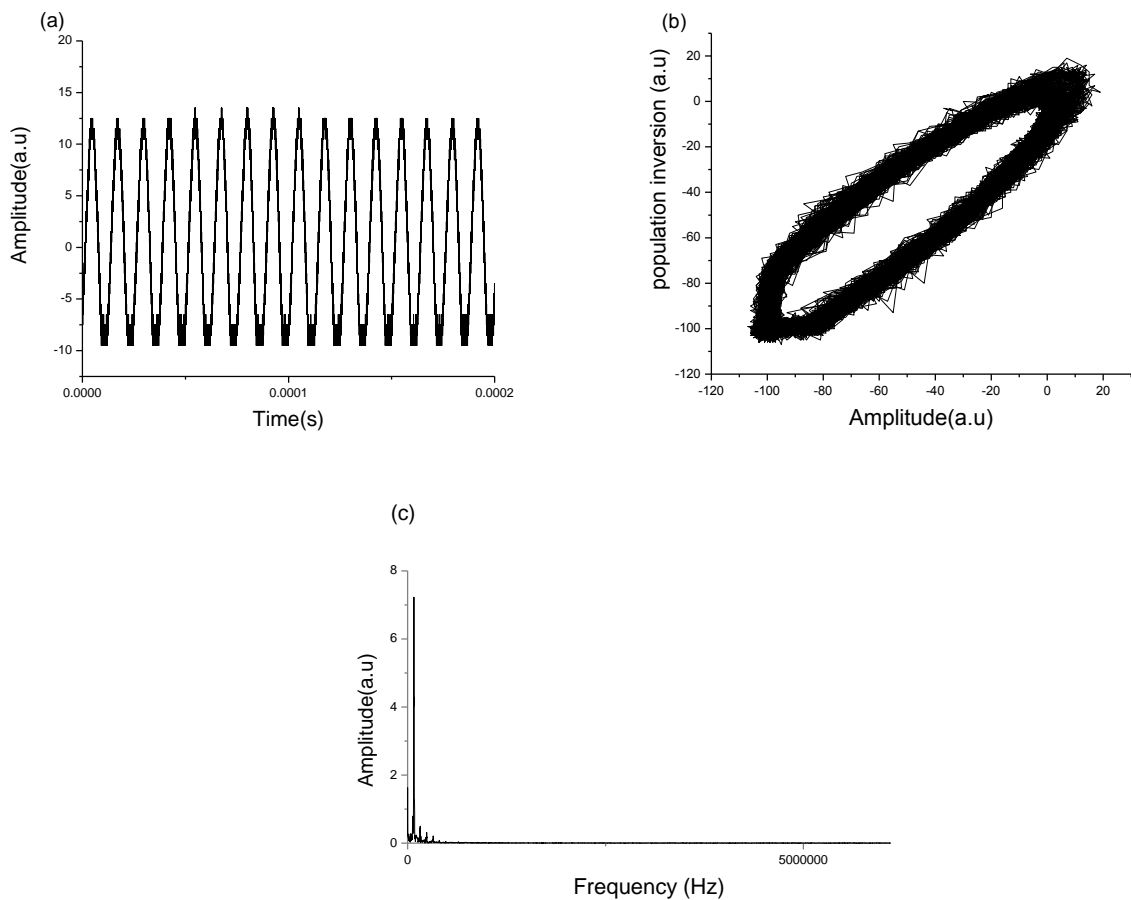


Figure 4.6 (a) the time series when $\varepsilon = 0.78$, (b) the corresponding FFT (c) the corresponding attractor.

FFT diagram shows very limited frequencies with one high amplitude peak as in figure 4.6(c). The corresponding attractor of this state is a limit cycle as in figure 4.6(b).

Increasing value of strength to $\varepsilon = 0.82$, the less periodic (quasi-periodic) state will be shown as in figure 4.7(a), while figure 4.7(c) represents the

corresponding FFT of this state. It is clear that the peaks with various intensities are very limited. The attractor shows this condition as well, figure 4.7(b). It is a quasi- limit cycle attractor.

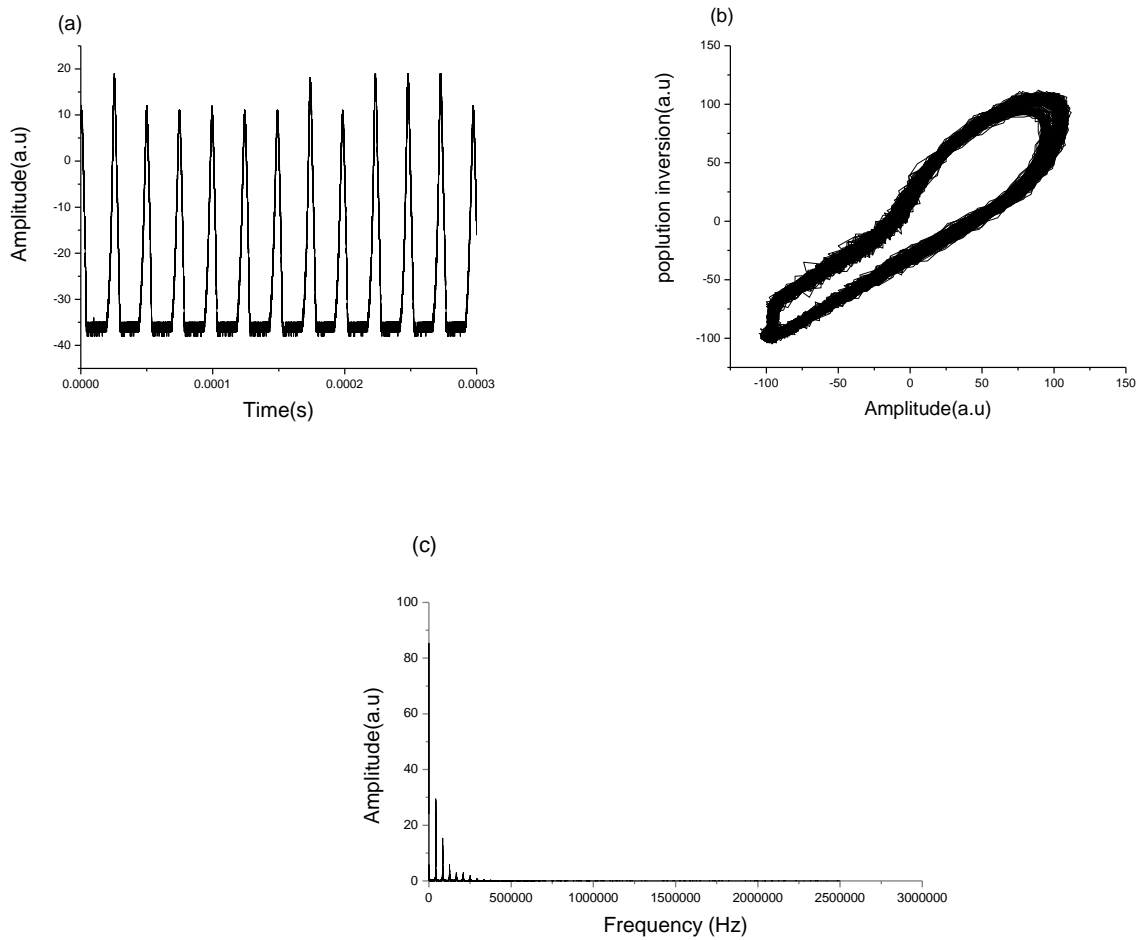


Figure 4.7 (a) the time series when $\varepsilon = 0.82$, (b) the corresponding FFT (c) the corresponding attractor.

In figure 4.8(a) the time series shows chaotic attain state and small branches in the oscillators of the output power spectrum when the feedback strength is ($\varepsilon = 0.94$). In figure 4.8(c) the corresponding FFT shows this state has high density peaks with difference amplitudes. The corresponding attractor of the state show more irregularity as in figure 4.8(b).

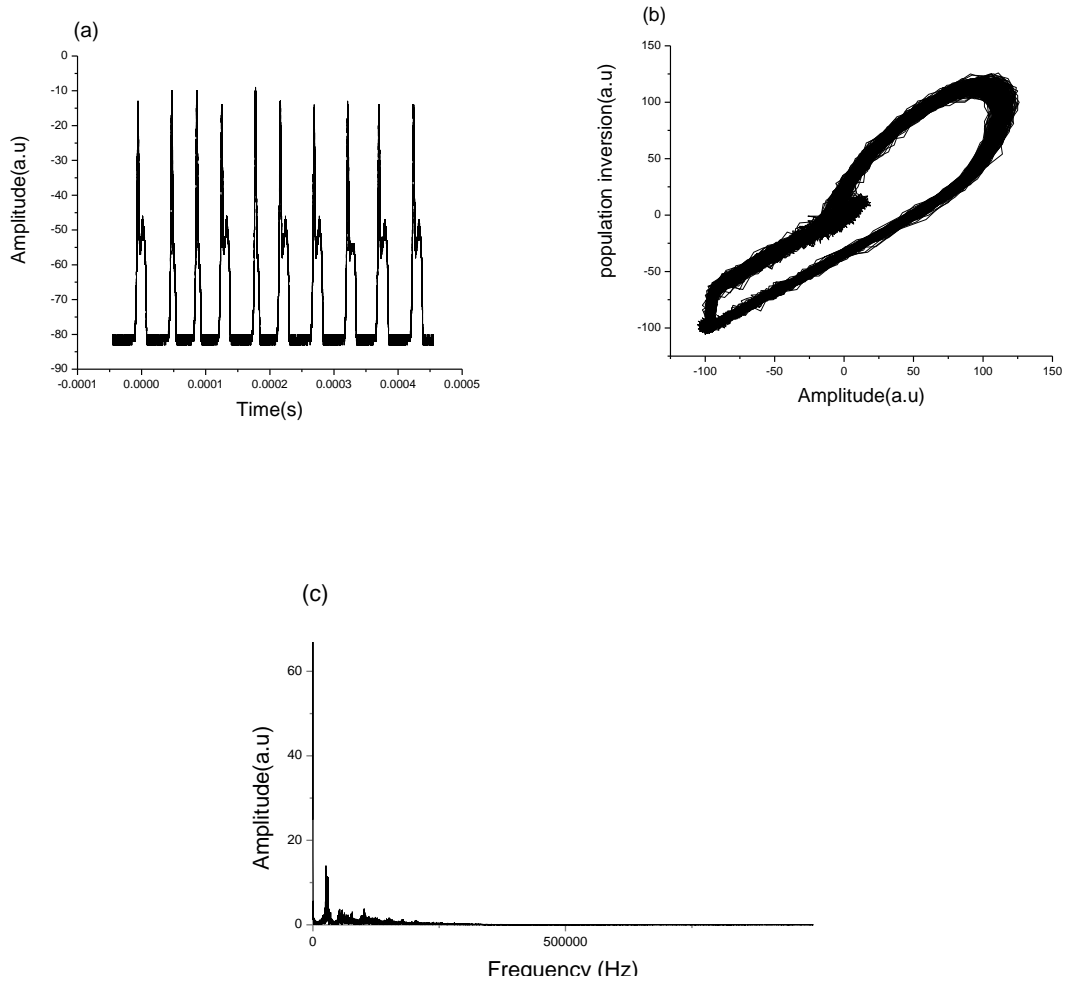


Figure 4.8(a) the time series when $\varepsilon = 0.94$, (c) the corresponding FFT, (b) the corresponding phase space (attractor).

We notice the figure 4.9(a) displayed the chaotic state as a result to the increasing of feedback strength to ($\varepsilon=1.32$) which is more irregularity than in figure 4.8(a). In corresponding FFT of this state we see much density peaks of varied frequency instead of exponential decay as in figure re 4.8(c) the corresponding attractor of this state shown in figure 4.9(b).

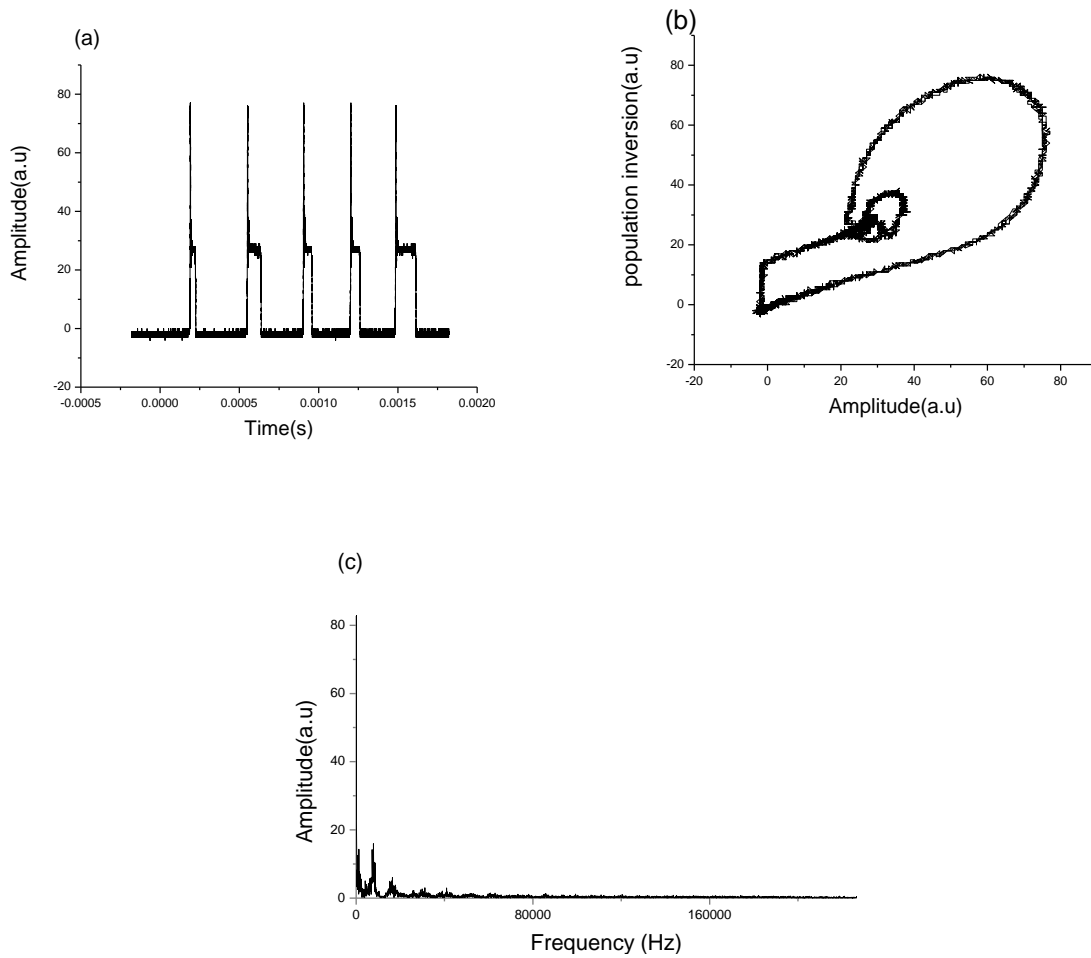


Figure 4.9(a) the time series when $\varepsilon = 1.32$, (b) the corresponding FFT, (c) the corresponding attractor.

The observed intensity spectra with the increase of the feedback strength (the values of the amplification) were being the definitive guide to say that the feedback strength is one of the most important parameters for generating chaotic situation in laser nonlinear systems via optoelectronic feedback, we notice that when the feedback strength increases the regime tumbles toward the unstable (chaotic) state wherever the bias current δ_o , is always constant.

4.2.1.3 Effect of Modulation on the Chaotic System

In the previous section the chaotic behavior in laser nonlinear dynamical systems was obtained by changing the value of the bias current while the value of the feedback strength (gain amplification) was being fixed, and vice-versa which indicated that the optoelectronic feedback is very important route to chaos. But in this section we would investigate the effect of the frequency modulation on the chaotic system, for that purpose we plotted the maxima recordings of the power of laser as a function of the frequency at a fixed value of amplitude modulation at 50mV. This frequency control diagram demonstrates the response of chaotic system versus frequency of the sinusoidal signal as shown by the Bifurcation diagram in the figure 4.10 below

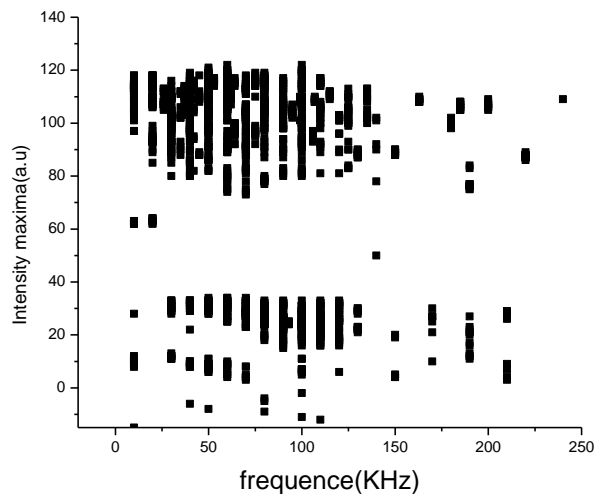


Figure 4.10: Experimental bifurcation diagram of the laser intensity as a function of the frequency modulation.

4.2.2 The Influences of Noise on the Chaotic System Behavior

4.2.2.1 Coherence Resonance Phenomenon

In this part of the work we aimed to demonstrate the effect of noise in our chaotic system, by investigating the role of external noise. When a Gaussian noise generator is inserted into the feedback loop, and starting driving the white noise of intensity from D equals $1\text{mV}_{(\text{rms})}$ to about $24\text{mV}_{(\text{rms})}$, here we can determine the behavior of our system due to additive noise to the bias current of the laser. When noise was added to the driving current of the laser, giving rise to a pulsed behavior in the laser output, in the form of the well known (LFF). The regularity of the dropout series initially increases with increasing noise level, and peaked for an optimal amount of noise as we notice later.

By applying a signal noise of intensity $D = 5.5\text{mV}$, on the regime of spiking chaos, (chaotic regime) corresponding to the optoelectronic feedback, the time series and its attractor of the dynamic system can represent by figure 4.11.

When the parameter D (noise intensity) is increased to $D = 9.5\text{mV}$ the spikes become more frequent, fig.4.12, and at $D = 12.5\text{mV}$ the behavior becomes almost periodic, fig.4.13. Further increase of noise level to $D = 24.5\text{mV}$ leads to irregular output signal, fig.4.14.

So the noise shows the surprising ability to increase level of periodicity in the output of the SL system. We can note clearly the influence of noise on the system behavior via the time series and attractor where there is an increasing of the number of spike with increasing the noise intensity and the orbit is closed to the saddle point in the attractor.

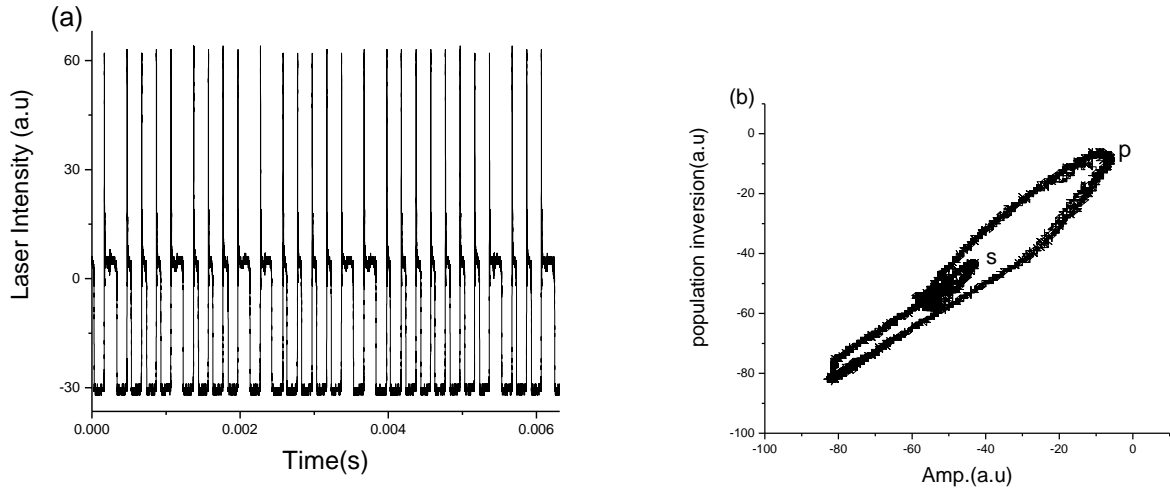


Figure 4.11: (a) Experimental time series of the semiconductor laser with feedback, (b) the corresponding Trajectory at noise of $D = 12.5\text{mV}$.

The spikes in time series in this figure displayed different amplitudes; and the phase trajectory which built by an embedding technique with appropriate delays, consists of a large regular loop plus a chaotic tangle around the saddle focus S. When the parameter D (noise intensity) is increased to $D = 9.5\text{mV}$ the spikes become more frequent, and the phase trajectory consists of a large regular loop plus, small periodic around the saddle focus, fig.4.12.

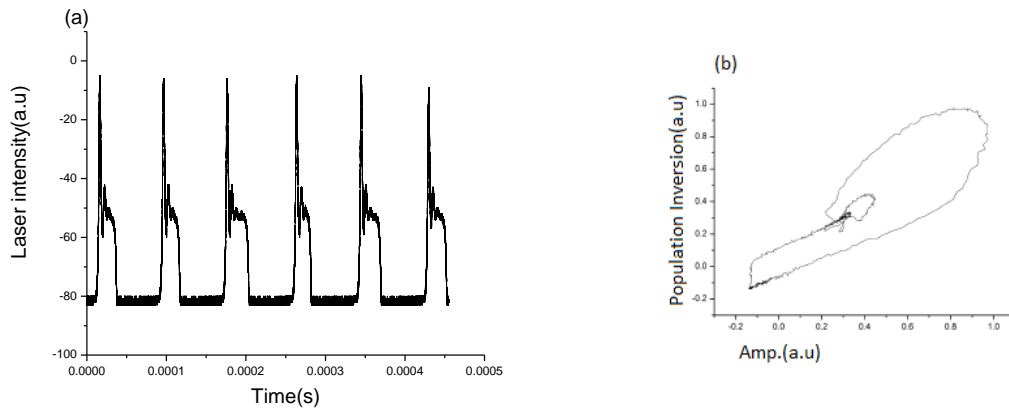


Figure 4.12: (a) Experimental time series of the semiconductor laser with feedback, (b) the corresponding Trajectory at noise of $D = 9.5\text{mV}$.

By increasing noise intensity to, $D = 12.5\text{mV}$ the behavior becomes almost periodic, and the phase trajectory consist of a large regular loop.fig.4.13.

So the noise shows the surprising ability to increase level of periodicity in the output of the SL system. We can note clearly the influence of noise on the system behavior via the time series and attractor where there is an increasing of the number of spike with increasing the noise intensity and the orbit is closed to the saddle point in the attractor.

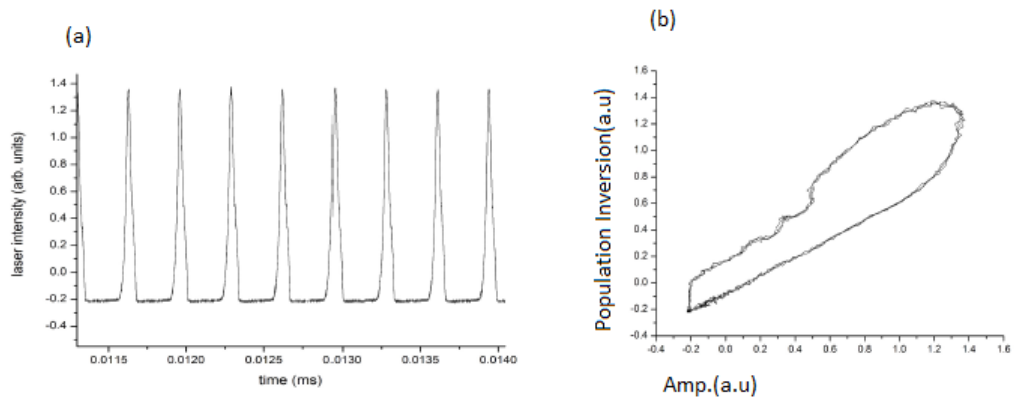


Figure 4.13: (a) Experimental time series of the semiconductor laser with feedback, (b) the corresponding Trajectory at noise of $D = 12.5\text{mV}$.

Further increase of noise level to $D = 24.5\text{mV}$ leads to irregular output signals, and the phase trajectory consist of a large regular loop plus small periodics around the saddle focus, fig.4.14.

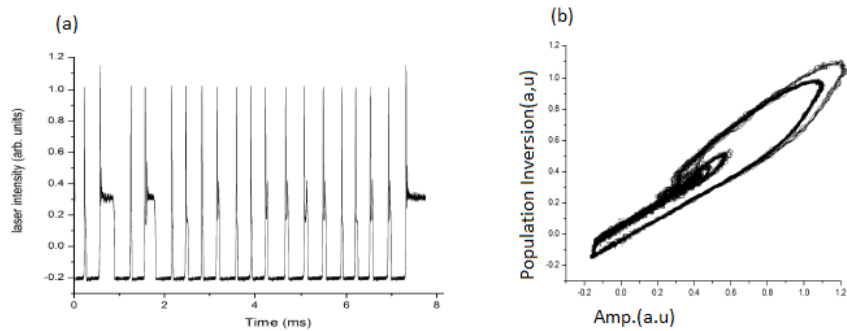


Figure 4.14: (a) Experimental time series of the semiconductor laser with feedback, (b) the corresponding Trajectory at noise of $D = 12.5\text{mV}$.

We can give a full description of the response of our regime with arbitrary white noise intensity by the bifurcation diagram which plotted in figure 4.15.

The points A, B and C are indicated to the figures 4.11, 4.13 and 4.14 respectively.

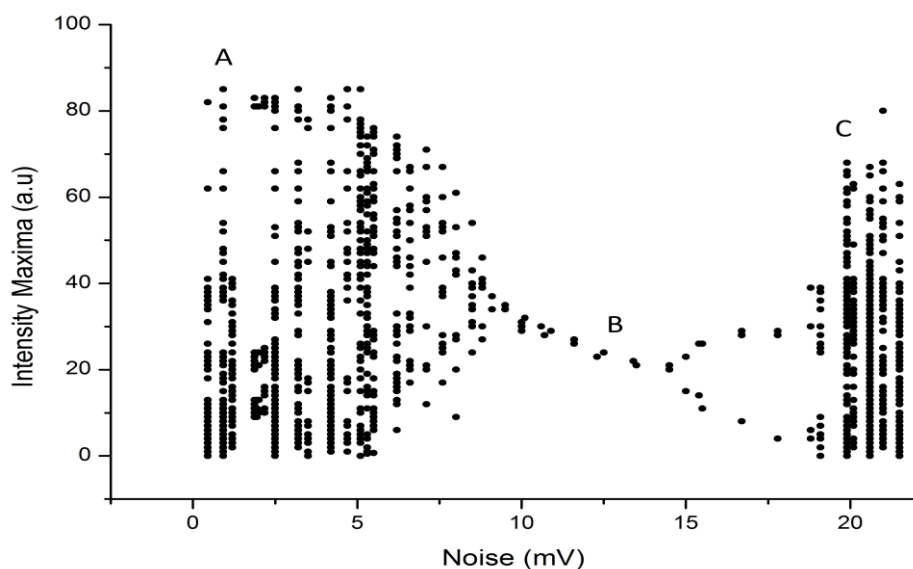


Figure 4.15 Experimental bifurcation diagrams as a function of noise intensity.

In chapter two we defined the activation time $t_{(a)}$ and the excursion time $t_{(e)}$ and interspike time-intervals (ISI), by using those definitions we measured the coefficient of variation R , which is given as the ratio of the standard deviation of interspike time-intervals from the corresponding mean value, to the mean value and plot as a function of noise intensity, Fig.4.16, at optimal noise intensity R has a minimum value. The occurrence of a minimum in the coefficient of variation (the standard deviation of the distribution of interspike intervals (ISI) normalized by its mean) for noise levels in between these extremes is considered as a key indication for coherence resonance. Also we plot the relation between the SNR and the intensity of noise, Fig.4.17, which is much related with the Fig.4.16; here SNR has a maximum at optimal noise intensity.

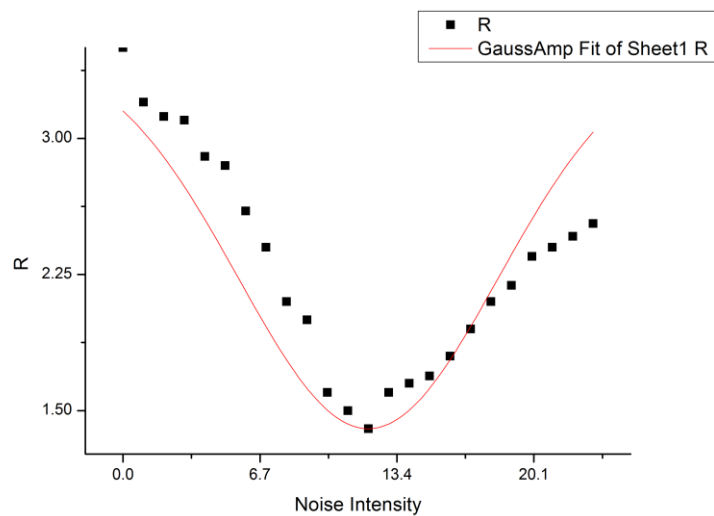


Figure 4.16: The coefficient of variation R as a function of noise intensity.

We can investigate the summary of the experimental results as follows: the small amount of noise produces infrequent dropouts, which become more numerous and regular as the noise amplitude increases. For large noise strengths the pulses become increasingly irregular, both in separation

and in amplitude. Hence, optimal amplitude of the external noise exists for which the coherence of the pulsed output of the laser is optimal.

From these results, we conclude that there exists optimal amplitude of external noise for which the output laser is almost periodic. It is apparent from Fig.4.13 that increasing of the noise level affects not only the duration of the pulses but also their amplitudes. This result confirms the idea that the irregularity of the pulse amplitude increases with noise. Thus, we predict that a semiconductor laser with a source of noise can display coherence resonance and it may be applied in network communications where the enhancement of regular pulses is required. The pulses could be obtained as a result of the interaction of the SL with the noise source.

Table (4.1): The Experimental values of noise intensity and NSR in the CR effect respectively.

Noise Intensity(mV) (X)	NSR (y)
0	0
2.5	0
5	0
7.5	0
8	100
10	700
12.5	920
15	730
16	410
22	200
25	100

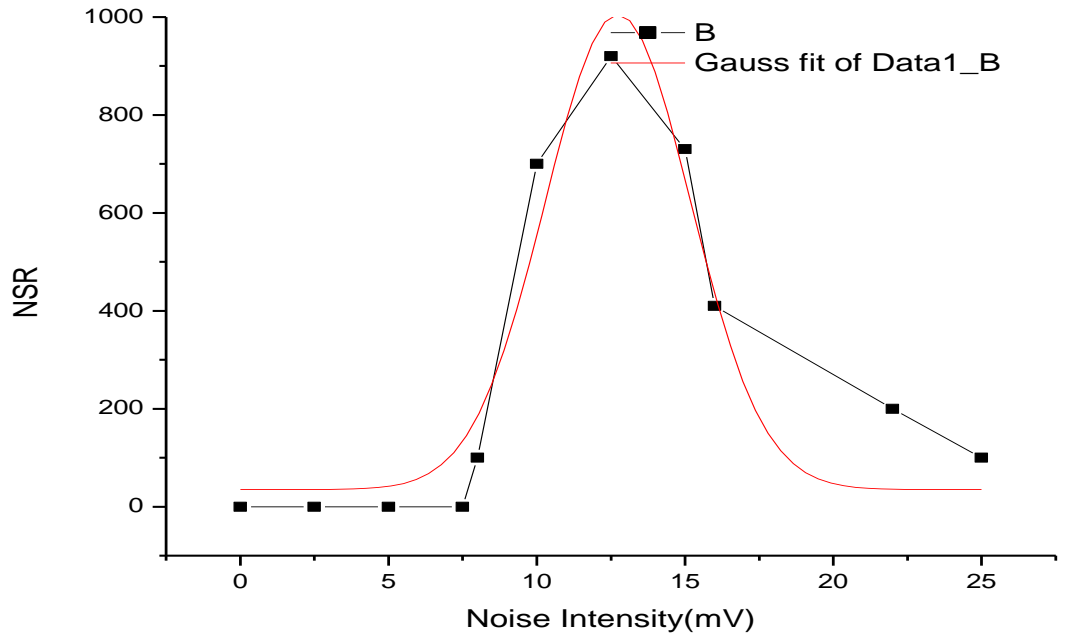


Figure 4.17: SNR as a function of noise intensity shows the coherence resonance at optimal noise intensity.

4.2.2.2 Stochastic Resonance Phenomenon

The noise in this experimental setup can enhance the response of the laser chaotic regime to a weak external periodic driving (signal), in a sort of stochastic resonant effect or phenomenon.

In this work we applied a weak sinusoidal signal of 200 KHz frequency to the feedback loop with a noise signal as it showed in Fig.4.18, which amplitude was systematically increased.

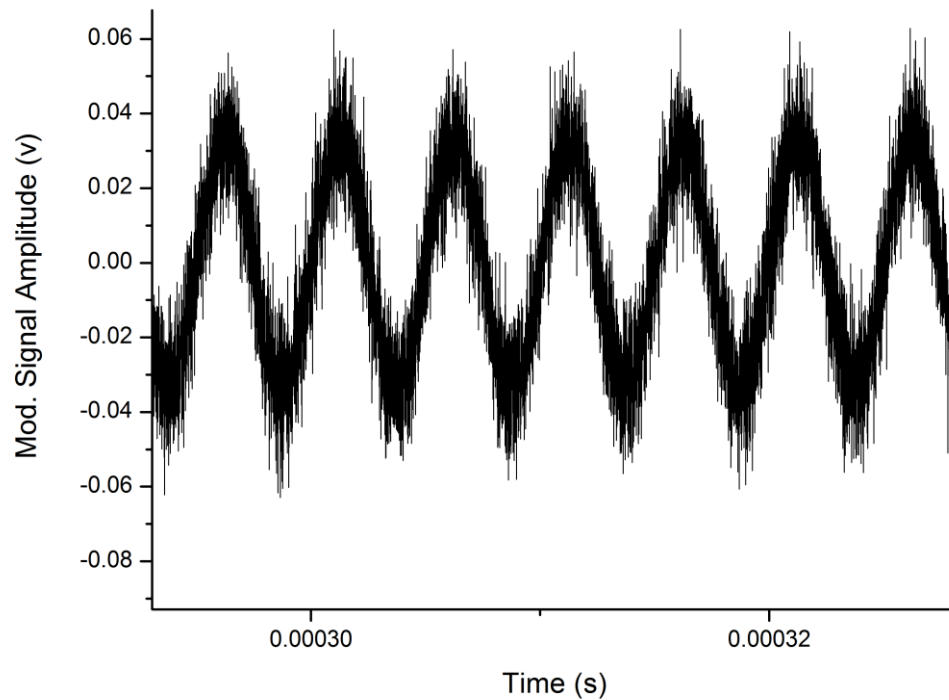


Figure 4.18: sinusoidal signal was modulated to the feedback loop with a noise signal

. For the different noise intensities, we observed different power spectra pattern with a sharp peak at the modulation period for certain noise levels Fig.4.19. Note in this figure the influence of the noise intensity as follows: at noise intensity ($D = 0$), the sinusoidal signal is fully hidden from the power spectrum, in fact; this is the importance of the chaos to encrypt data in optical communications, where data disappear when modulated in a chaos carrier. When the noise intensity was increased the sinusoidal signal is began to appear in the power spectrum as a sharp peak, Fig.4.19 (b), and continue to increase in amplitude with increasing the intensity of the noise, Fig.4.19(c) until reaches to the maximum at an optimal value of the intensity of noise, at this point the stochastic resonance phenomenon was achieved, Fig.4.19(c). The word resonance in the term stochastic resonance was originally used because the signature feature of SR is that a plot of a

performance measure such as output SNR against input noise intensity. When further increase of the intensity of the noise, the peak of the sinusoidal signal is drops and disappear again, Fig.4.19 (d).

The SNR of the peak for increasing values of noise amplitude is presented in Fig.4.20. We can observe how the SNR had a maximum for intermediate values of noise, which is reflected in the power spectrum as a well defined peak at the modulation frequency. This maximum is the typical signature of SR.

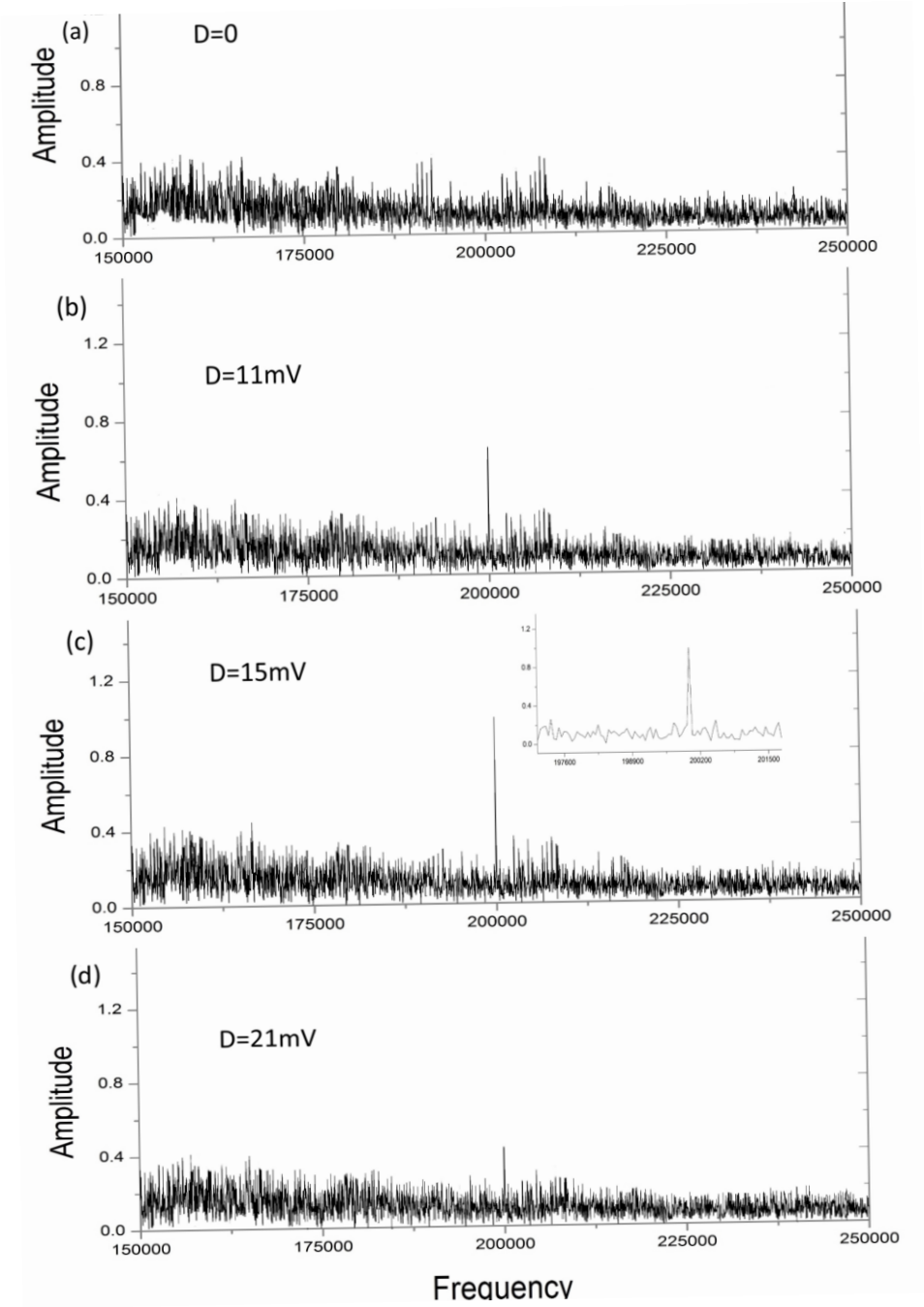


Figure4.19: The increasing of the signal power spectrum as a function of the values of noise intensity.

From the figure 4.19, we note that the maximum signal-to-noise ratio is obtained for intermediate values of noise intensity (c), decreasing for higher noise intensities (d).

Table (4.2): The Experimental values of noise intensity and NSR in SR effect respectively.

Noise Intensity(mV) (X)	SNR (Y)
0	-23
4	-24.5
10	-17
11	-15
15	-12.5
17.5	-16
22	-20
22.5	-23
25	-25

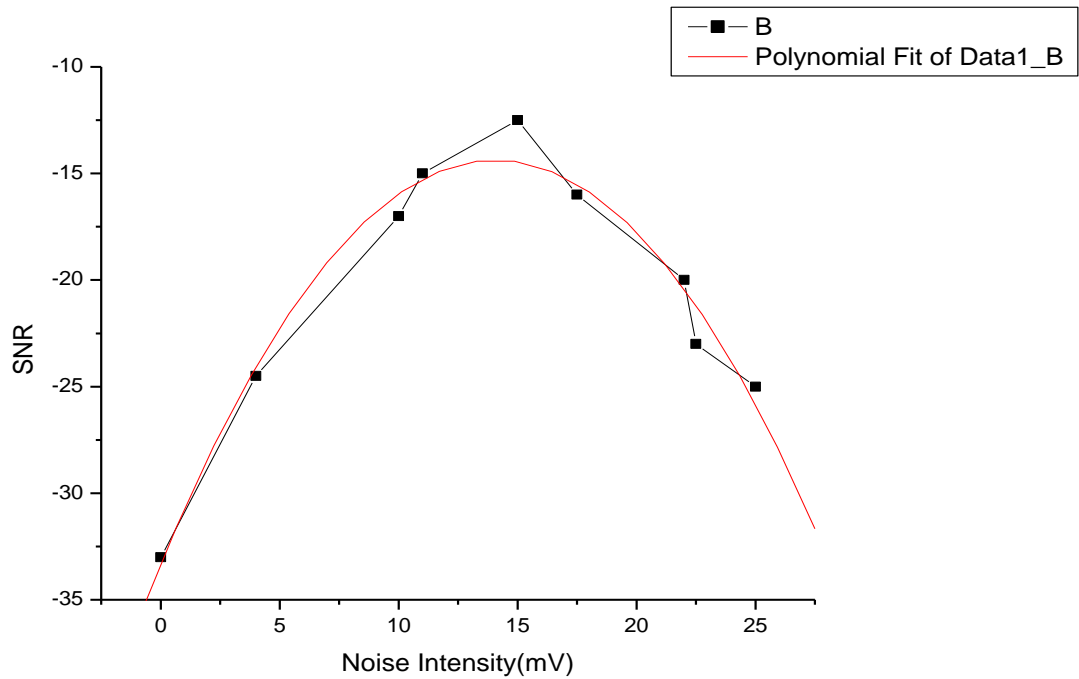


Figure 4.20: Experimental results for the signal to noise ratio as a function of the noise value.

4.3 Conclusion

In conclusion, we have experimentally studied the generation of chaos dynamics using semiconductor laser (LD), by means of optoelectronic feedback.

The analysis of the chaotic generation is presented, showing the generation of the mixed spectrum in the time series and the attractor.

The dependence of the injected current on the feedback fraction is observed.

Coherence resonance (CR) and stochastic resonance (SR) phenomena occurs due to noise bridging different configurations of bistable or multistable systems.

CR refers to coherence motion stimulated by optimal noise (perturbation) on the intrinsic dynamics of the system without the presence of the external periodic forcing (signal).

SR happens when the signal-to-noise ratio (SNR) of a dynamical nonlinear chaotic laser diode regime increases, for intermediate value of the noise intensity (D).

4.4 Suggestion for Future work

To duce more complexity of the chaotic carrier, there are some suggested works which are:-

1. Studying full synchronization between two chaotic oscillators in unidirectional and bidirectional configurations.
2. Two optical feedback, branches could be injected in nonlinear dynamical system, like MZM; the first branch could be injected to the RF input of the MZM, while the second branch could be injected to the laser system. This configuration may offer high dynamical spiking rates.
3. Multi loop OEO, using fiber length to OEO, cavity to reduce the limitation of the electrical band pass filter, which removes unwanted side modes from the signal, the an increasing of the fiber length, the spacing between the cavity modes decreases and by using high quality electrical band filter, this could lead some non- oscillating side modes.

References

1. Abdalah, S. F. (2013) *Dynamical systems*. PhD lectures notes, Sudan University of Science and Technology, Laser Institute, Sudan, Khartoum.
2. Abdalah, S. F., Al-Naimee, K.A. and Meucci R. (2010) *Experimental Evidence of Slow Spiking Rate in a Semiconductor Laser by Electro-Optical Feedback: Generation and Control*. Applied Physics Research, Vol. 2, No. 2, pp. (170-175).
3. Abdalah, S.F. Ciszak, M. , Marino, F. , Al-Naimee, K.A. , Meucci, R. , Arecchi, F.T. (2012) *Noise effects on excitable chaotic attractors in coupled light emitting diodes*. Browse Journals & Magazines Systems Journal, IEEE Volume:6 Issue:3
4. Abraham, R. and Ueda, Y. (2000) *The Chaos Avant grade, Memories of the Early Days of Chaos Theory*. World scientific, London.
5. AliceProject, Available at, http://en.wikipedia.org/wiki/Chaos_theory
6. Al-Naimee, K. Marino, F. Ciszak, M. Meucci, R. and Arecchi, F. T. (2009). *Chaotic spiking and incomplete homoclinic scenarios in semiconductor lasers with optoelectronic feedback*. New Journal of Physics, vol. 11.
7. Al-Naimee, K. Marino, F. Ciszak, M. Abdalah, S. F. Meucci, R. and Arecchi, F. T. (2010) *Excitability of periodic and chaotic attractors in semiconductor lasers with optoelectronic feedback*. Eur. Phys. J. D, vol. 58, pp. 187-189.

8. Ando, B. and Graziani, S. (2000) *Stochastic Resonance Theory and Applications*. Kluwer Academic Publishers, Boston, London.
9. Arecchi, F. and Meucci, R. (2009) *Stochastic and coherence resonance in lasers: homoclinic chaos and polarization bistability*. Eur. Phys. J. B 67.
10. Arecchi, F.T. and Meucci, R. (2009) *Stochastic and Coherence Resonance in Lasers: Homoclinic Chaos and Polarization Bistability*. Eur. Phys. J. B 69.
11. Arecchi, F. T., Meucci, R. and Gadomski, W. (1986) *Generation of Chaotic Dynamics by Feedback on a Laser*. Phys. Rev. A34, pp.1617-1620.
12. Argyris, A. et al. (2005) *Spectral Synchronization in Chaotic Optical Communication Systems*. IEEE J. Quantum Electron. vol. 41, no. 6, pp. 892-897.
13. Aström, K. J., and Murray, R.M. (2008) *Feedback Systems An Introduction for Scientists and Engineers*. Copyright by Princeton University Press.
14. Avila, M. et al. (2004) *Deterministic coherence resonance in semiconductor lasers*. 8th Experimental Chaos Conference. AIP Conference Proceedings, vol. 742, pp. 253-260.
15. Benzi, R. et al. (1981) *The mechanism of stochastic resonance*. J. Phys. A14.
16. Bodova, k. (2009) *Topics in Applied Stochastic Dynamics*. Ph. D. thesis, University of Michigan.
17. Buldu, J. M. et al. (2004) *External noise in semiconductor lasers*. Proc. of SPIE, vol. 5468, pp. 118-132.
18. Burada, P. S. et al. (2008) *Entropic stochastic resonance," Phys. Rev. Lett. 101*.

19. Cao, L. and Wu, D. J. (2007) *Stochastic resonance in a single-mode laser driven by quadratic colored pump noise: Effects of biased amplitude modulation signal*. Phys. A 376.
20. Chapeau, F. and Blondeau, (2000) *Stochastic Resonance and the Benefit of noise in Nonlinear Systems*. Lecture Notes in Physics, Vol. 550, pp. 137-155, Springer Berlin.
21. Clayton, K. (1997) *Basic Concepts in Nonlinear Dynamics and Chaos*. Marquette University, Milwaukee, Wisconsin, Keith Clayton.
22. Collins, J., Chow, C. and Imho, T. (1995) *Stochastic resonance without tuning*. Nature, vol. 376, p. 236.
23. Devi, M. and Shinde, A.A.(2013) *Signal Analysis of Real Time Signals to Remove Noise*. International Journal of Engineering and Advanced Technology (IJEAT) ISSN: 2249 – 8958, Volume-3, Issue-1.
24. Dhobale, S., Boldhan, V. and Burange, R.A. (2013) *Implementation of Adaptive Noise Canceller using LMS Algorithm*. National Conference on Innovative Paradigms in Engineering and Technology (NCIPET), published by International Journal of Computer Applications (IJCA).
25. Douglass, J. K. et al. (1993) *Noise enhancement of information transfer in crayfish mechanoreceptors by stochastic resonance*. Nature.
26. Du, L. C. and Mei, D. C. (2009) *The effects of time delay on stochastic resonance in a bistable system with correlated noises*. Chin. Phys. B 18.
27. Dykman, M. I. et al. (1991) *Stochastic resonance in an all-optical passive bistable system*. Journal of Experimental and Theoretical Physics Letters 53, p. 193.

28. Fauve, S and Heslot, F. (1983) *stochastic resonance in a bistable system*. Physics Letters A 97.
29. Fiber Optic Association (1999- 2013) *Guide To Fiber Optic and Premises Cabling*. Published by FOA, Inc.
30. Gammaiton, L. et al. (1998) *stochastic resonance*. Reviews of Modern Physics, Vol. 70, No. 1.
31. Gammaitoni, L. (1995) *Stochastic Resonance and the Dithering Effect in Threshold Physical Systems*. Phys. Rev. E 52 (5): 4691–8.
32. Gammaitoni, L. et al. (1998) *Stochastic resonance*. Reviews of Modern Physics, vol. 70, no. 1, p. 223.
33. Giacomelli, G. et al. (2000) *Experimental evidence of coherence resonance in an optical system*. Phys. Rev. Lett. 84.
34. Hibbs, A. D. et al. (1995) *Stochastic resonance in a superconducting loop with a josephson junction*. Journal of Applied Physics 77.
35. Hilbom, R.C. (2004) *A simple model for stochastic coherence and stochastic resonance*. Am. J. phys. 72,528.
36. Hirsch, M. W., Smale, S. and Devaney R. L (2004) *Differential equations, dynamical systems, and an introduction to chaos*. Elsevier
37. Ian, P. (1998) *Thermal Noise Tutorial*. University College London, UK.
38. Iooss, G., Ropert, H. G. and Stora, R. (1983) *Chaotic Behavior of Deterministic Systems*. Amsterdam .N.Y., North-Holand.
39. Jia, Y., Yu, S. N. and Li, J. R. (2000) *Stochastic resonance in a bistable system subject to multiplicative and additive noise*. Phys. Rev. E 62.

40. Jin, Y. and Haiyan, (2007) *Coherence and Stochastic Resonance in a Delayed Bistable System*. Physica A 382, pp, 423–429, copyright by Elsevier B.V.
41. Jung, P. and Hanggi, P. (1989) *Stochastic nonlinear dynamics modulated by external periodic force*. Europhys. Lett., vol. 8, no. 6, pp. 505-510.
42. Kaneko, K. and Tsuda, I. (2001) *Complex Systems: Chaos and Beyond a Constructive Approach with Applications in Life Sciences*. university of Tokyo, Japan.
43. Keizer, J. (1988) *Statistical thermodynamics of nonequilibrium processes*. Copyright by Springer, Verlage.
44. Kosko, and Bart, (2006) *Noise*. Viking, New York.
45. Lawrence, J. S. (2000) *Diode lasers with optical-feedback, optical-injection, and phase-conjugate feedback*. PhD Thesis, Macquarie University.
46. Liu, J., Chen, H. and Tang, S. (2001) *Optical Communication Systems Based on Chaos in Semiconductor lasers*. IEEE Transactions on Circuits and Systems, vol. 48, no. 12, pp. 1475-1483.
47. Liu, Y. and Ohtsubo, J. (1994) *Experimental Control of Chaos in a Laser-Diode Interferometer with Delayed Feedback*. Vol. 19, No. 7, pp. (448-450).
48. Locher, M. Inchiosa, M. E. Neff, J. Bulsara, A. Wiesenfeld, K. Gammaitoni, L. Hanggi, P. and Ditto, W. (2000) *Theory of controlling stochastic resonance*. Phys. Rev. E, vol. 26, no. 1, pp. 317-327,

49. Luo, X., and Zhu, S. (2003) *Stochastic resonance driven by two different kinds of colored noise in a bistable system*. Phys. Rev. E 67.
50. McNamara, B., k. and Roy, R. (1988) *Observation of Stochastic Resonance in a Ring Laser*. Phys. Rev. Lett. 60, 2626.
51. Mork, J., Tromborg, B. and Mark, J. (1992) *Chaos in Semiconductor Lasers with Feedback: Theory and Experiments*. IEEE J. Quantum Electron. Vol., 28, pp. (93-107).
52. Moss, F., Ward, L.M. and Sannita, W.G. (2004) *Stochastic Resonance and Sensory Information Processing: a Tutorial and Review of Application*. Clinical Neurophysiology 115 (2): 267–81, Elsevier.
53. Nicolis, C. (1982) *Stochastic aspects of climatic transitions responses to periodic forcing*. Tellus 34.
54. Ohtsubo, J. (2008) *Semiconductor Lasers Stability, Instability and Chaos Second Enlarged Edition*. Shizuoka University, Springer-Verlag Berlin Heidelberg.
55. Ohtsubo, J. (2013) *Semiconductor Lasers Stability, Instability and Chaos. Third Edition*. Springe.
56. Ott, H. W. (1988) *Noise Reduction Techniques in Electronic Systems*. Second Edition John Wiley and Sons.
57. Palenzuela, C. et al. (2001) *Coherence Resonance in Chaotic Systems*. Department of Physics, Lehigh University - Bethlehem, PA 18015, USA.
58. Palonpon, A. et al. (1998) *Measurement of Weak Transmittances by Stochastic Resonance*. Optics Letters 23 (18): 1480–2.

59. Pieroux, D. and Mandel, P. (2003) *Bifurcation Diagram of a Complex Delay Differential Equation with Cubic Nonlinearity*. Physical review E67.
60. Pikovsky, A. S. and Kurths, J. (1997) *Coherence Resonance in a Noise-Driven Excitable System*. Physical Review Letters, Volume 78, Number 5, the American Physical Society.
61. Ravindranadh, K. Rao, M. C. (2013) *Fundamental Approach to Clinical Applications of Intense Pulsed Light*. Journal of Intense pulsed lasers and applications in advanced physics Vol. 3, No. 4, p. 47 – 50.
62. Romero, N. A. (1998) *Johnson noise*. Junior Physics Laboratory, Massachusetts Institute of Technology, Cambridge, Massachusetts 02139.
63. Rontani, D. and Citrin, D.S. (2005) *Introduction to Chaos*. Department of Physics, Duke University, Durham-North Carolina.
64. Russell, D. F., Wilkens, L. A. and Moss, F. (1999) *Use of behavioural stochastic resonance by paddle fish for feeding*. Nature.
65. Scholl, E. and Schuster, H.G. (2008). *Handbook of Chaos Control*. 2nd Ed, Wiley-VCH Verlag GmbH and Co. KGaA, Weinheim ISBN.
66. Silfvast, W. T. (2004) *Laser fundamentals*. Copyright by William T.Silfvast.UK.
67. Sobering, T. J. (1999) *Noise in Electronic Systems*. Technot 4, copyright by Tim J. Sobering.
68. Solorio, J. M.S. et al. (2002) *Bifurcation in a Semiconductor Laser Subject to Delayed Incoherent Feedback*. Optics Communications 214, pp.(327–334).

69. Spano, M. L., Wun-Fogle, M. and Ditto, W. L. (1992) *Experimental observation of stochastic resonance in a magnetoelastic ribbon*. Physical Review A 46.
70. Strogatz, S.H. (1994) *Nonlinear Dynamics and Chaos with Applications to Physics, Biology, Chemistry and Engineering*. Perseus Books Publishing, L.L.C.
71. Szucs, A. et al. (2003) *Synaptic Modulation of the Inter spike Interval Signatures of Bursting Pyloric Neurons*. Copyright by the American Physiological Society.
72. Tang, S. and Liu, J. M. (2001) *Chaotic Pulsing and Quasi-Periodic Route to Chaos in a Semiconductor Laser with Delayed Opto-Electronic Feedback*. IEEE J. Quantum Electron. vol. 37, no. 3, pp. 329-336.
73. Tredicce, J. R. et al. (1985) *Instabilities in lasers with an injected signal*. J Opt Soc Am B 2.
74. Ward, L.M. et al. (2006) *Neural Synchrony in Stochastic Resonance Attention, and Consciousness*. Can J Exp Psychol 60 (4): 319–26.
75. Wellens, T., Shatokhin, V and Buchleitner, A. (2004) *Stochastic Resonance*. Rep. Prog. Phys. 67. 45–105, IOP Publishing Ltd, UK.
76. Wu, D., Zhu, S. and Luo, X. (2009) *Spatially correlated diversity induced resonance*. Phys. Rev. E 79.
77. Xu, Y. et al. (2013) *Levy noise-induced stochastic resonance in a bistable system*. The European Physical Journal B, vol. 86, p. 198.
78. Zhang, H., Liu, D. and Wang, Z. (2009) *Controlling Chaos, Suppression, Synchronization and Haptification*. Springer-Verlag, London.

79. Zhao, L. et al. (2010) *Entropic stochastic resonance driven by colored noise*. Chin. Phys. Lett. 27.